JOURNAL OF NEUROTRAUMA 29:1982–1998 (July 1, 2012)

DOI: 10.1089/neu.2011.2253

In Vitro Stretch Injury Induces Time- and Severity-Dependent Alterations of STEP Phosphorylation and Proteolysis in Neurons

Mahlet N. Mesfin,[1] Catherine R. von Reyn,[1] Rosalind E. Mott,[1] Mary E. Putt,[2] and David F. Meaney[1,3]

Abstract

Striatal-enriched tyrosine phosphatase (STEP) has been identified as a component of physiological and pathophysiological signaling pathways mediated by *N*-methyl-D-aspartate (NMDA) receptor/calcineurin/calpain activation. Activation of these pathways produces a subsequent change in STEP isoform expression or activation via dephosphorylation. In this study, we evaluated changes in STEP phosphorylation and proteolysis in dissociated cortical neurons after sublethal and lethal mechanical injury using an *in vitro* stretch injury device. Sublethal stretch injury produces minimal changes in STEP phosphorylation at early time points, and increased STEP phosphorylation at 24 h that is blocked by the NMDA-receptor antagonist APV, the calcineurin-inhibitor FK506, and the sodium channel blocker tetrodotoxin. Lethal stretch injury produces rapid STEP dephosphorylation via NR2B-containing NMDA receptors, but not calcineurin, and a subsequent biphasic phosphorylation pattern. $STEP_{61}$ expression progressively increases after sublethal stretch with no change in calpain-mediated $STEP_{33}$ formation, while lethal stretch injury results in $STEP_{33}$ formation via a NR2B-containing NMDA receptor pathway within 1 h of injury. Blocking calpain activation in the initial 30 min after stretch injury increases the ratio of active STEP in cells and blocks $STEP_{33}$ formation, suggesting that STEP is an early substrate of calpain after mechanical injury. There is a strong correlation between the amount of $STEP_{33}$ formed and the degree of cell death observed after lethal stretch injury. In summary, these data demonstrate that previously characterized pathways of STEP regulation via the NMDA receptor are generally conserved in mechanical injury, and suggest that calpain-mediated cleavage of $STEP_{33}$ should be further examined as an early marker of neuronal fate after stretch injury.

Key words: altered signal transduction; *in vitro* studies; neural injury; traumatic brain injury

Introduction

Traumatic brain injury (TBI) resulting from a primary blunt or diffuse insult to the brain is a leading cause of death worldwide, with 1.7 million reported cases and 52,000 deaths each year in the United States alone (Faul et al., 2010). The primary mechanical trauma to the brain activates secondary signaling cascades responsible for the widespread and long-lasting motor, cognitive, and behavioral deficits observed in TBI patients (Pierce et al., 1998; Raghupathi, 2004; Smith et al., 1997). Determining the mechanisms that regulate secondary signaling propagation is critical to understanding how to minimize the extent of the initial injury, and to develop therapeutics to improve functional outcome after TBI. Glutamate receptors act as significant sensors of the initial mechanical injury during TBI, showing both immediate and more prolonged changes in receptor physiology, receptor subtype expression, and relative number of synaptic receptors (Bell et al., 2007; Kumar et al., 2002; Osteen et al., 2004; Schumann et al., 2008; Spaethling et al., 2008; Zhang et al., 1996). Combined with a post-acute increase in extracellular glutamate levels following trauma (Faden et al., 1989; Palmer et al., 1993), the role of glutamate receptors remains important for several hours, if not days, after the initial injury (Miller et al., 1990; Osteen et al., 2004; Sun et al., 2008). A critical glutamate receptor activated by TBI is the *N*-methyl-D-aspartate receptor (NMDAR), a tetraheteromeric structure composed of two NR1 and two NR2 subunits, which are primarily the NR2A and NR2B subunits in cortical and hippocampal neurons (McIntosh et al., 1990; Monyer et al., 1994).

[1]Department of Bioengineering, [2]Biostatistics and Epidemiology, and [3]Department of Neurosurgery, University of Pennsylvania, Philadelphia, Pennsylvania.

TBI causes a loss of the voltage-gated magnesium block that normally limits calcium influx through the NMDAR, resulting in hyperactivation of the NMDA response in neurons after injury (Geddes-Klein et al., 2006b; Hori and Carpenter, 1994; Paoletti and Ascher, 1994; Zhang et al., 1996). While NMDAR antagonists show promise in preclinical studies of TBI, they exhibit poor efficacy in clinical trials (Ikonomidou and Turski, 2002; Loane and Faden, 2010). This illustrates the central challenge of developing glutamate receptor-based therapies for TBI, as even more targeted inhibition of glutamate receptor subtypes may disrupt their broader role in normal physiological function, such as neurotransmission, synaptic plasticity, and cell survival (Akashi et al., 2009; Bliss and Collingridge, 1993; Hardingham et al., 2002; Liu et al., 2007).

An alternative therapeutic approach for TBI targets specific signaling networks downstream of the pathophysiological activation of glutamate receptors to directly modulate cues to preferentially promote neuronal repair, regrowth, and even regeneration. Kinases and phosphatases represent ideal target proteins for these alternative therapies, as they are reversible control points for switching on and off signaling networks (Hardingham et al., 2002; Lee et al., 2005). Much of the work in understanding phosphorylation-mediated signaling for the design of therapeutic strategies for TBI has focused on kinases, therefore less is known about how specific phosphatases shape neuronal fate after traumatic injury. One phosphatase activated by NMDA-mediated calcium influx is striatal-enriched tyrosine phosphatase (STEP), an alternatively spliced phosphatase enriched in the striatum, cortex, and hippocampus of the brain (Boulanger et al., 1995; Paul et al., 2003). The full-length STEP isoform, $STEP_{61}$, is enriched in the ER membrane and the post-synaptic density (PSD), while another dominant isoform, $STEP_{46}$, has a cytoplasmic distribution throughout the cell (Boulanger et al., 1995; Bult et al., 1997). Three signaling pathways converge on STEP as a substrate: protein kinase A (PKA) activation, which phosphorylates Ser49/221 on STEP to render it unable to bind to its substrates (Paul et al., 2000); calcineurin activation, which dephosphorylates STEP and allows it to bind to its substrates (Paul et al., 2003); and calpain activation, which cleaves $STEP_{61}$ to form the inactive isoform $STEP_{33}$ (Nguyen et al., 1999; Xu et al., 2009). When activated, STEP mediates numerous physiological pathways through ERK, p38 kinase, and Fyn dephosphorylation, as well as dephosphorylates the NR2B subunit, leading to internalization of the NMDA receptor (Braithwaite et al., 2006; Nguyen et al., 1999; Paul and Connor, 2010; Paul et al., 2003; Poddar et al., 2010; Snyder et al., 2005; Xu et al., 2009). STEP also regulates endocytosis of the AMPA receptor and limits the induction of long-term potentiation (Pelkey et al., 2002; Zhang et al., 2008,2010), and $STEP_{61}$ expression is decreased via ubiquitination through synaptic NMDAR activation, or rapidly increased via translation (Hu et al., 2007; Kurup et al., 2010; Paul et al., 2007; Xu et al., 2009; Zhang et al., 2008). Alternatively, STEP plays a role in the pathophysiological signaling triggered by excitotoxicity, ischemia, Alzheimer's disease, seizures, Huntington's disease, and drug abuse (Braithwaite et al., 2008; Briggs et al., 2011; Choi et al., 2007; Hicklin et al., 2011; Kurup et al., 2010; Saavedra et al., 2011; Xu et al., 2009; Zhang et al., 2010). In all, STEP possesses three main characteristics that make it a likely target for study in TBI: (1) activation linked to calcium dysregulation occurring in traumatic injury; (2) altered availability of functional protein after proteolysis, a common feature of TBI (Pike et al., 1998); and (3) influence on downstream signaling pathways commonly studied in TBI (Atkins et al., 2007,2009; Kumar et al., 2002; Raghupathi et al., 2003; Schumann et al., 2008).

The specific role of STEP in TBI is unknown, particularly in determining whether STEP influences cell survival or modulates neural networks after trauma. In this study, we investigate changes and mechanisms of STEP phosphorylation and proteolysis in cortical neurons using a model of *in vitro* mechanical stretch injury. This injury model provides a rapid mechanical strain to dissociated neurons in a uniaxial and strain-dependent manner, producing a robust and transient NMDAR-mediated calcium influx into neurons (Geddes-Klein et al., 2006a; Lusardi et al., 2004; Spaethling et al., 2008). We hypothesized that STEP is activated in cortical neurons following stretch injury through an NMDAR- and calcineurin-dependent pathway. We show that there is a time-, strain-, and activity-dependent component to the changes in STEP phosphorylation and proteolysis following stretch injury, which are mediated by activation of NMDAR and calpain, respectively. In addition, cell death following stretch injury was significantly reduced, but not eliminated, with NMDAR antagonists, and correlated strongly with the extent of calpain-mediated STEP proteolysis at 24 h after injury. However, neither the initial STEP dephosphorylation nor neuronal death was altered by the calcineurin antagonist FK506. Together, these data exhibit the complex regulation of STEP following stretch injury, while suggesting that $STEP_{33}$ formation may be a critical early calpain substrate that can determine long-term neuronal fate after injury.

Methods

Generation of phospho-STEP antibody

A phospho-specific STEP antibody was generated by Covance Technologies (Denver, PA). Briefly, immunizing peptides were designed based on an 18-amino acid sequence [CKKKSMGLQERRG–pS–NVSLTLD] within the KIM domain of $STEP_{61}$, which contained the phosphorylated Ser49/221 residue as indicated. New Zealand white rabbits were repeatedly inoculated with the phospho-peptide conjugated to KLH, and samples from periodic production bleeds were analyzed for their titer and specificity to phosphorylated STEP. After 110 days, the animals were sacrificed and the terminal serum from one rabbit was affinity purified using peptides based on a non-phosphorylated immunizing sequence, followed by affinity purification with peptides for the phospho-immunizing sequence. The affinity-purified phospho-antibody was evaluated for its specificity against the control peptide in various applications, including *in vitro* assays, Western blotting, immunoprecipitation, immunocytochemistry, and immunohistochemistry.

Purification of GST-STEP constructs

pGEX-2T plasmid containing the $STEP_{46}$ sequence was obtained from the Lombroso Lab (Yale University, New Haven, CT). These plasmids were transformed into TOP10 competent cells (Invitrogen, Carlsbad, CA), which were grown to mid-log phase and GST-STEP protein production was induced with 0.5 mM IPTG. After 16–18 h, the resulting protein was purified

with the B-PER GST Purification Kit (Pierce Biotechnology, Rockford, IL) following the manufacturer's instructions. The concentrations of the purified GST-STEP proteins were determined with the Bradford DC protein assay (Bio-Rad, Hercules, CA), and the protein was stored at −80°C until use.

Phosphorylation and dephosphorylation of recombinant GST-STEP

Purified recombinant GST-$STEP_{46}$ was tested for its ability to be phosphorylated using a modified version of a previously described method (Paul et al., 2003). Briefly, equal amounts of STEP protein were incubated with and without 1–2 μg of purified PKA (Sigma-Aldrich, St. Louis, MO) for 30 min at 30°C. The reaction was terminated by adding 1×SDS sample buffer (Invitrogen), and boiling the sample for 5 min at 95°C. For experiments with calpain, the same protocol was followed, except PKA was heat-inactivated at 65°C for 20 min, and 5 U calpain (Calbiochem, Gibbstown, NJ), and 2.5 μM $CaCl_2$ were added to the reaction mixture for 30 min at room temperature. The reaction was stopped by adding 1×SDS sample buffer and boiling at 95°C for 5 min.

Primary dissociated neuronal cultures

All animal procedures were completed in accordance with the University of Pennsylvania Institutional Animal Care and Use Committee. All materials were obtained from Invitrogen Corporation unless otherwise noted. Embryos at day E18 were removed via cesarean section from a pregnant Sprague-Dawley rat anesthetized with 5% CO_2 and sacrificed via cervical dislocation. Cortices were isolated from the embryos in calcium- and magnesium-free Hank's balanced salt solution and incubated for 15 min at 37°C in trypsin (1.4 mg/mL) and DNAse (0.6 mg/mL; Roche Applied Science, Indianapolis, IN). After trituration and filtration, the cells were resuspended in plating medium (MEM with Earl's salts and GlutaMAX™ supplemented with 0.6% D-glucose [Sigma-Aldrich], 1% Pen-Strep, and 10% horse serum). The cells were plated on poly-D-lysine- (0.01 mg/mL; Sigma-Aldrich), and laminin- (0.001 mg/mL; BD Biosciences, San Jose, CA) coated surfaces at a density of $0.2–0.5\times10^6$ cells, and incubated at 37°C in 5% CO_2. For studies with the *in vitro* stretch injury model, the cultures were plated on deformable silicone membranes (Sylgard 184 and 186; Dow Corning, Midland, MI). After 24 h, the plating medium was removed and replaced with feeding medium (Neurobasal™ media supplemented with B-27 and 0.4 mM GlutaMAX™). The cells were treated with 1 μM arabinofuranosyl cytidine (Sigma-Aldrich) in the feeding medium from days *in vitro* (DIV) 4 to DIV 8 to inhibit the proliferation of glial cells in the cultures. Feeding medium was replenished every 3–4 days and cultures were maintained for 16–21 DIV until use. This culturing time was chosen in order to create a mature glutamatergic receptor profile (Lin et al., 2002), and to limit the amount of synaptic "chatter" that appears before DIV 12 (Opitz et al., 2002), as these oscillations can affect the neuronal response to mechanical injury (Geddes-Klein et al., 2006b).

Stretch injury on dissociated neurons

At DIV 16–20, feeding medium was replaced with Neurobasal-based saline solution (NBS) (media composition, in mM: 100 NaCl, 5.4 KCl, 0.8 $MgCl_2$, 1.8 $CaCl_2$, 26 $NaHCO_3$, 0.9 NaH_2PO_4, 10 HEPES, 0.01 glycine, and 25 glucose, pH 7.4). The cells were subjected to a strain-controlled stretch injury as described previously (Lusardi et al., 2004). Briefly, cells plated on deformable membranes were inserted into a closed pressure chamber. A controlled air pressure pulse was injected into the chamber, causing the membrane to deflect through a rectangular opening (2×18 mm), and mechanically injure the cells only within this rectangular region. The applied deformation (defined by the peak stretch in percent) was uniform over 95% of the stretched membrane surface area. The magnitude of the stretch injury was calibrated to the applied input pressure for each week of experiments, and a transducer recorded the applied output pressure of each test (Endevco, San Juan Capistrano, CA). This resulting output pressure can be correlated with similar magnitude and strain rates observed in animal models of TBI (Meaney et al., 1995). After the pressure-induced injury, the cultures were placed back in the incubator for the duration of the experiment. At the desired time post-injury, cells were lysed in lysis buffer (in mM: 50 Tris-HCl, 150 NaCl, 2 EDTA, 0.25% NP-40, complete mini [Roche Applied Science], 1 sodium vanadate, 0.05 NaF, and 0.01 potassium permanganate, pH 7.6). For injured samples, cells from the rectangular region of stretch were isolated and lysed separately, in order to exclusively collect only cells that underwent injury. Lysates were briefly sonicated, centrifuged at 16000*g* for 15 min at 4°C to remove unlysed material, and the nuclear fraction, and the supernatants were stored at −80°C until use.

NMDA stimulation of dissociated neurons

For NMDA stimulation experiments, 100 μM NMDA in NBS was added to the cultures for the desired time and lysed as described above.

Drug treatments

For the antagonist and inhibitor studies, drugs were added to the saline solution 15–30 min before injury, and remained on the cells for the course of the experiment. In a subset of 24-h cultures, the drug was rinsed off and replaced with saline solution 30 min after stretch injury. APV (25 μM; Sigma-Aldrich), a competitive NMDA-receptor antagonist, and FK506 (1 μM; LC Labs, Woburn, MA), a calcineurin inhibitor, were used to block all NMDA receptor and calcineurin activity, respectively. To block NR2B-containing NMDA receptors, the NR2B subunit antagonist Ro 25-6981 (10 μM) was used (Fischer et al., 1997), and to block synaptic activity, the sodium channel blocker tetrodotoxin (TTX; 1 μM; Tocris, Ellisville, MO) was used.

Immunoprecipitation

Samples were lysed in lysis buffer (in mM: 50 Tris-HCL, 150 NaCl, 0.5% NP-40, complete mini [Roche Applied Science], 1 sodium vanadate, 0.05 sodium fluoride, and 0.01 potassium pyrophosphate), centrifuged at 16000*g* for 15 min at 4°C, and equal protein amounts were incubated with protein-Sepharose G beads (Invitrogen), and spun for 1.5 h at 4°C to pre-clear samples. Five micrograms of anti-STEP antibody (Santa Cruz Biotechnology, Santa Cruz, CA) were added to the pre-cleared lysates and spun overnight at 4°C. Fresh

protein-Sepharose G beads were added to the lysate and antibody solution for 2 h at 4°C, and the beads were rinsed four times in lysis buffer + 0.1% NP40. Protein was eluted from the beads with SDS sample buffer (Invitrogen) at 95°C for 5 min, and processed for Western blotting.

Electrophoresis and Western blotting

Protein concentrations of lysates were determined using the Bradford protein assay kit (Bio-Rad). Equal amounts of protein were denatured in sample buffer + 2.5% βME for 5 min at 95°C and run on 4–12% Bis-Tris (Invitrogen), transferred onto PVDF membranes, blocked in 5% dry milk, and probed with the antibody of interest overnight at 4°C. Antibodies used in this study include mouse anti-STEP (1:250; Santa Cruz Biotechnology), rabbit anti-p-STEP (1:5000; Covance), rabbit anti-p-CREB (1:3000; Cell Signaling, Boston, MA), rabbit anti-CREB (1:2000; Cell Signaling), mouse anti-actin (1:10,000; Millipore, Billerica, MA), and mouse anti-spectrin (1:10,000; Millipore). The blots were then rinsed and incubated with secondary HRP antibodies, incubated with ECL reagents (Pierce Biotechnology), and the bands were visualized by exposure to film. The blots were stripped and re-probed with the panel of antibodies listed above, and the results were quantified using a computer-assisted two-dimensional densitometry scanning program (Kodak 1D Image Analysis Software; Eastman Kodak Company, Rochester, NY). All band intensities were normalized to a time-matched, uninjured/unstimulated sample from that week of experiments. A drug effect of APV was observed in the baseline levels of STEP phosphorylation in our cultures, therefore all injured, drug-treated samples were normalized to uninjured drug controls from that week of experiments. To quantify the relative amount of phosphorylated STEP in the cultures, we calculated the ratio of the normalized intensity of the phospho-STEP band divided by the normalized intensity of the $STEP_{61}$ band. To quantify changes in total $STEP_{61}$ or phospho-STEP levels, we calculated the ratio of normalized intensity of STEP band over the normalized intensity of the actin band. To quantify changes in total $STEP_{33}$, the samples were normalized to the untreated, 80% injured sample, instead of the untreated, uninjured controls.

Assessment of cell death

Cells were injured as described above and placed in an incubator at 37°C in 5% CO_2. Twenty-four hours after injury, the cells were incubated in 20 μg/μL Hoescht 33342 (Invitrogen) and 2 μM ethidium homodimer (Invitrogen) in NBS (pH 7.4) for 30 min in the incubator to examine the extent of cell death after injury (Spaethling et al., 2008). The cells were rinsed twice with NBS and imaged on a Nikon TE300 microscope equipped with a UV and a Texas Red filter. For each uninjured control well, images from three fields of view were collected. For each injured well, images were taken from three fields of view within the injured region of cells, and two fields of view within an adjacent, uninjured region. A code created in Matlab (MathWorks, Natrick, MA) was used to determine the number of total cells in the well (Hoescht-positive), the number of dead cells in the well (ethidium homodimer-positive), and the number of cells that co-labeled with both dyes (EthHD-positive). A ratio of the number of co-labeled cells divided by the number of Hoescht-positive cells was calculated, and this percent EthHD-positive value was reported as a percent of cell death in that well. The values for cell death were normalized to the values for cell death in saline, 80% injured samples from that week of experiments. At least three wells were imaged for each condition, and injured wells were excluded from further analysis if cell death within the non-injured regions was greater than 30%.

Statistical analysis

Data are described using means ± standard error of the mean (SEM) unless otherwise stated. Either one-way or two-way analysis of variance (ANOVA) with an interaction between the two factors was used to assess the overall significance of the model. In the one-way ANOVA, we tested the significance ($p < 0.05$) of injury at each time point versus shams. In the two-way ANOVA, if the interaction term was found to be significant ($p < 0.05$), we tested the significance of drug versus control at each stretch level. In the two-way ANOVA with main effects, we tested for significant between-individual levels of each factor. The statistical analysis was performed using JMP (SAS Institute, Cary, NC) or the R stats package (http://www.r-project.org). Regression analysis was performed using Microsoft Excel.

Results

Characterization of phospho-STEP antibody

The phosphorylation state of a serine residue (Ser49/Ser221) on STEP regulates its activity; phosphorylation of this residue by PKA prevents STEP binding to its substrates and produces an inactive form of STEP (Paul et al., 2000,2003). To directly visualize changes in STEP activity in the cells, we generated a phospho-specific antibody against a peptide sequence on STEP containing the Ser49/Ser221 residue, and tested its specificity with a series of *in vitro* assays using purified recombinant GST-$STEP_{46}$ and PKA. Western blots revealed an immunoreactive band at the correct molecular weight when PKA-phosphorylated STEP was probed with the phospho-STEP antibody (Fig. 1A). No band appeared in samples that were not incubated with PKA. Co-incubation of the antibody with the immunizing phospho-peptide attenuated the phospho-STEP signal (Fig. 1A). Adding a broad-specificity phosphatase, calf intestinal phosphatase (CIP), to the reaction mixture led to a dose-dependent loss of the phospho-specific band intensity (Fig. 1B). Although no change was observed in the total amount of STEP in the samples, a slight upward shift in band mobility was observed in samples containing PKA-phosphorylated STEP, which was reversed with the addition of CIP (Fig. 1B).

To test the utility of the phospho-STEP antibody in dissociated cortical neurons, we stimulated cells with NMDA (100 μM), and probed for changes in STEP phosphorylation as measured with the phospho-antibody. As previously reported (Paul et al., 2003), we observed a significant decrease in the ratio of phospho-$STEP_{61}$:total $STEP_{61}$ (phospho-STEP:-STEP) by 5 min that persisted for at least 30 min after NMDA stimulation (Fig. 1C and D). The mobility of the total $STEP_{61}$ band gradually shifted downward in parallel with the change detected with the phospho-STEP antibody. The ratio of phospho-STEP:STEP increased at 60 min, owing to a loss of total $STEP_{61}$ expression and low levels of phospho-STEP (Fig.

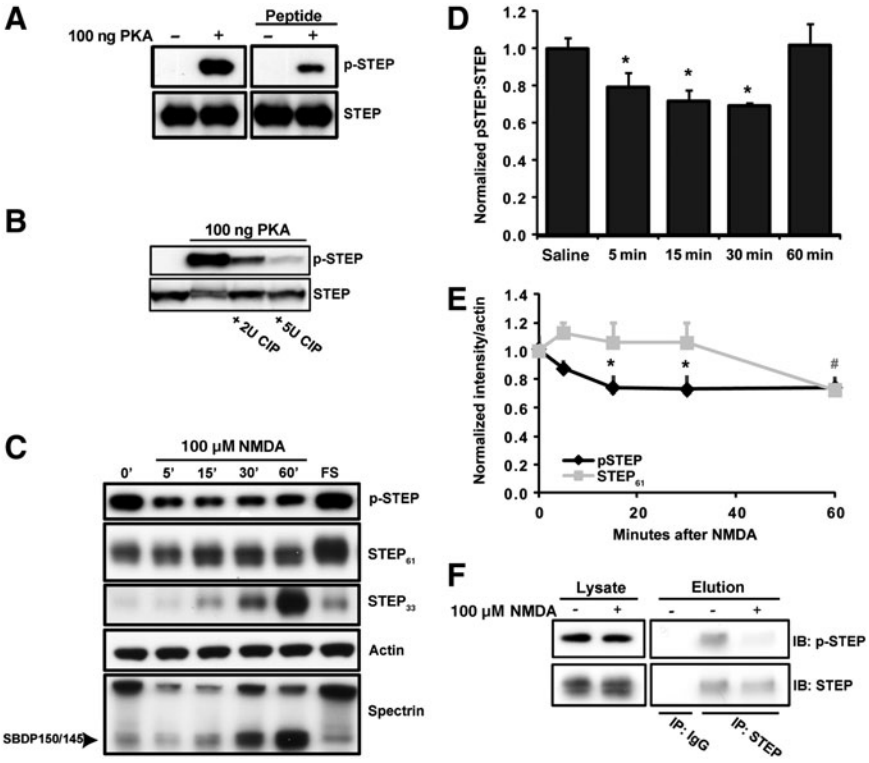

FIG. 1. Phospho-STEP antibody recognizes phosphorylated forms of recombinant and native STEP. (**A**) When probed with the phospho-antibody, recombinant GST-$STEP_{46}$ protein reveals a protein band only after incubation with PKA. Co-incubation of the antibody with the immunizing peptide attenuates the phospho-band intensity in identical blots. (**B**) Calf intestinal phosphatase (CIP) produces a dose-dependent decrease in the phospho-band intensity. (**C**) Dissociated cortical neurons stimulated with NMDA (100 μM) for increasing time periods, or with forskolin (FS; 20 μM for 60 min), were lysed and analyzed via Western blotting ($n = 3–6$/group). (**D**) Quantification shows a loss of the phospho-STEP:STEP ratio, and (**E**) a concurrent decrease in phospho-STEP (p-STEP) and $STEP_{61}$ levels after stimulation. (**F**) Immunoprecipitation of cortical neurons with an anti-STEP antibody reveals a protein band in the elution fraction when probed with the phospho-STEP antibody. The intensity of this band decreased after NMDA stimulation in the same pattern as in whole cell lysates ($n = 4$). All band intensities are normalized to time-matched, saline controls, and expressed as the indicated ratios. All values are presented as means ± standard error of the mean (*$p < 0.05$ versus saline or 0 min [p-STEP]; #$p < 0.05$ versus 0 min [$STEP_{61}$]; STEP, striatal-enriched tyrosine phosphatase; NMDA, *N*-methyl-D-aspartate; PKA, protein kinase A; SBDP, breakdown products of spectrin; IP, immunoprecipitation; IB, immunopositive band).

1E). Moreover, cells stimulated with forskolin, a PKA activator, also demonstrated enhanced STEP phosphorylation after 60 min (FS; Fig. 1C). A decrease in total $STEP_{61}$ expression produced by NMDA stimulation and its concurrent $STEP_{33}$ formation occurred on a similar time scale with calpain-specific breakdown products of spectrin (SBDP150/145 kDa; Fig. 1C).

STEP exhibits strong homology with other members of its protein tyrosine phosphatase (PTP) family. Therefore we wanted to verify that the phospho-band detected in cortical lysates was specific for STEP. Elution fractions from immunoprecipitations on cortical neurons with a total STEP antibody showed immunopositive bands corresponding to those detected in whole-cell lysates with the phospho-STEP antibody (Fig. 1F). Additionally, the NMDA-mediated STEP dephosphorylation detected in the elution fractions of the immunoprecipitations corresponded to the dephosphorylation measured in whole-cell lysates. Combined, these results demonstrate that the phospho-STEP antibody recognizes a STEP-specific band in cortical lysates, and can detect stimuli-mediated changes in STEP phosphorylation.

STEP phosphorylation and cleavage after in vitro *injury are dependent on time and severity*

After verifying the utility of the phospho-STEP antibody, we used the antibody to measure changes in STEP phosphorylation after *in vitro* stretch injury of cortical neurons. We injured cells at two severities: a 50% peak stretch level that does not cause neuronal death at 24 h after injury, and an 80% peak stretch level that results in death at that time (Geddes-Klein et al., 2006a; Spaethling et al., 2008). Measurements of phospho-STEP, $STEP_{61}$, and $STEP_{33}$ at different time points after stretch injury show progressive changes in STEP activity and proteolysis after injury (Fig. 2). Following 50% injury, no significant changes in STEP phosphorylation were apparent until an increase occurred at 24 h post-injury (Fig. 2C). In the same samples, $STEP_{61}$ expression rose steadily toward a peak at 6 h post-injury (Fig. 2D), before returning to baseline levels by 24 h post-injury. $STEP_{33}$ proteolysis was unchanged in the first 24 h after sublethal stretch injury (Fig. 2E), suggesting minimal calpain activation as evident by the lack of calpain-specific spectrin proteolysis in the same samples (data not shown).

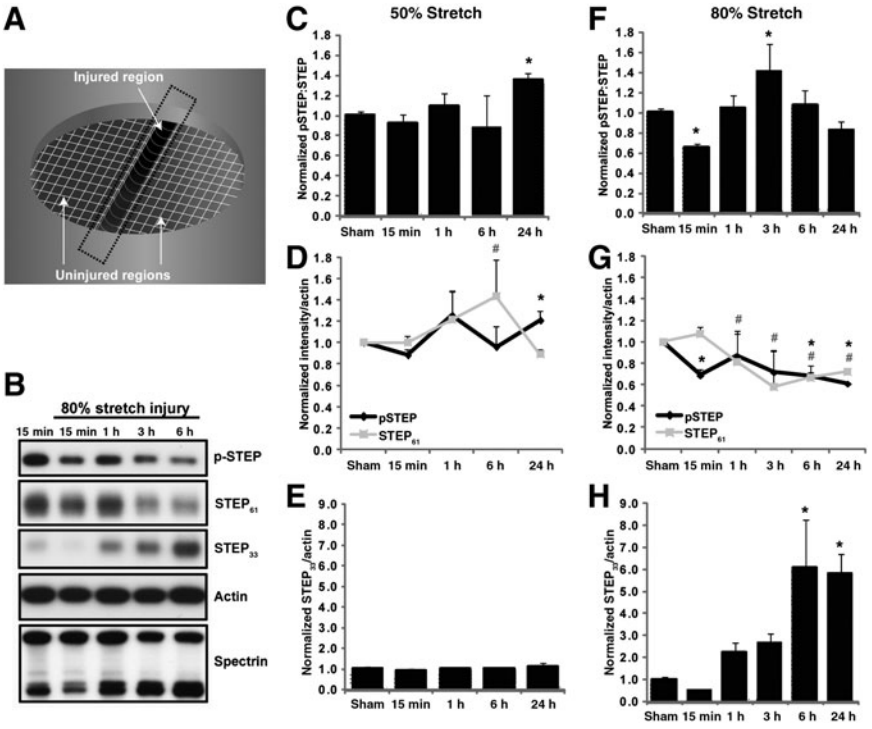

FIG. 2. Injury of cortical neurons at 50% and 80% stretch levels produces divergent changes in STEP phosphorylation and expression. (**A**) Schematic diagram of the membrane surface of the culturing well illustrates the injured region of the membrane (as it is displaced through a slit underneath the membrane), and the adjacent uninjured regions. Dissociated cortical neurons were injured at 50% and 80% peak stretch levels and cells were lysed at the indicated time points post-injury. (**B**) A representative Western blot shows the changes in STEP and phospho-STEP (p-STEP) in the injured cells (the area within the dotted lines in **A**) over time after 80% injury. Quantification of the band intensities after 50% (**C**–**E**; $n = 5$–23) and 80% stretch injury (**F**–**H**; $n = 9$–19) reveals that 50% injury increased STEP phosphorylation 24 h post-injury, and that 80% injury produces a biphasic STEP phosphorylation pattern. Injury at a 50% stretch level results in steadily increasing $STEP_{61}$ expression and no $STEP_{33}$ formation, while 80% injury produces a loss of $STEP_{61}$ expression and an increase in $STEP_{33}$ formation. All band intensities are normalized to time-matched, uninjured samples, and expressed as the indicated ratios. All values are presented as means ± standard error of the mean (*$p < 0.05$ versus sham [p-STEP]; #$p < 0.05$ versus sham [$STEP_{61}$]; STEP, striatal-enriched tyrosine phosphatase).

Following 80% stretch injury, a distinct pattern of STEP phosphorylation emerged. Within 15 min, STEP was significantly dephosphorylated and returned to control levels by 1 h post-injury (Fig. 2F and G). In turn, STEP phosphorylation significantly increased 3 h post-injury, before returning to slightly below baseline levels at 24 h after injury. At this time, $STEP_{61}$ expression progressively decreased while levels of $STEP_{33}$ increased, suggesting proteolytic degradation of $STEP_{61}$ by calpain (Nguyen et al., 1999), as evident by calpain-specific spectrin breakdown product formation along a similar time course in these samples (Fig. 2B and H). Taken together, these data indicate that patterns of STEP phosphorylation after stretch injury are influenced by the severity of mechanical injury, the relative proteolysis of $STEP_{61}$, and the time after injury.

Phosphorylation state of STEP alters its calpain cleavage in dissociated neuronal cultures

Although calcium influx is the common trigger for changes in STEP phosphorylation and proteolysis (Paul et al., 2003; Xu et al., 2009), it is not known if STEP phosphorylation influences the cleavage of STEP. We first used an *in vitro* recombinant protein assay to phosphorylate GST-$STEP_{46}$ with PKA and subsequently added calpain. Activation of calpain (with Ca^{2+}) significantly decreased the amount of full-length STEP, while increasing immunoreactivity of smaller STEP isoforms (Fig. 3A). However, no significant differences were detected in the extent of full length STEP cleavage in the presence or absence of PKA. Therefore, using an *in vitro* system, we show that PKA-mediated phosphorylation of STEP does not affect the susceptibility of STEP to be cleaved by calpain.

To examine if STEP proteolysis affects its pattern of phosphorylation after stretch injury in dissociated cortical neurons, we pretreated cells with the calpain inhibitor MDL-28170 (5 μM, 15 min) prior to stretch injury and examined STEP phosphorylation and proteolysis after 6 h. We selected this time point based on previous results from our lab showing that the cleavage of another calpain substrate, the α-subunit of the sodium channel, occurs by 6 h after stretch injury using this model (von Reyn et al., 2009). Six hours after 80% stretch injury, the formation of $STEP_{33}$ was completely blocked with continuous treatment with MDL-28170 (Fig. 3B and E). In addition, blocking $STEP_{61}$ proteolysis with MDL-28170 results in a further decrease in the phospho-STEP:STEP ratio 6 h after injury, with no change in total phospho-STEP (Fig. 3B–D), suggesting that dephosphorylated STEP may be preferentially cleaved after stretch injury in cultured neurons.

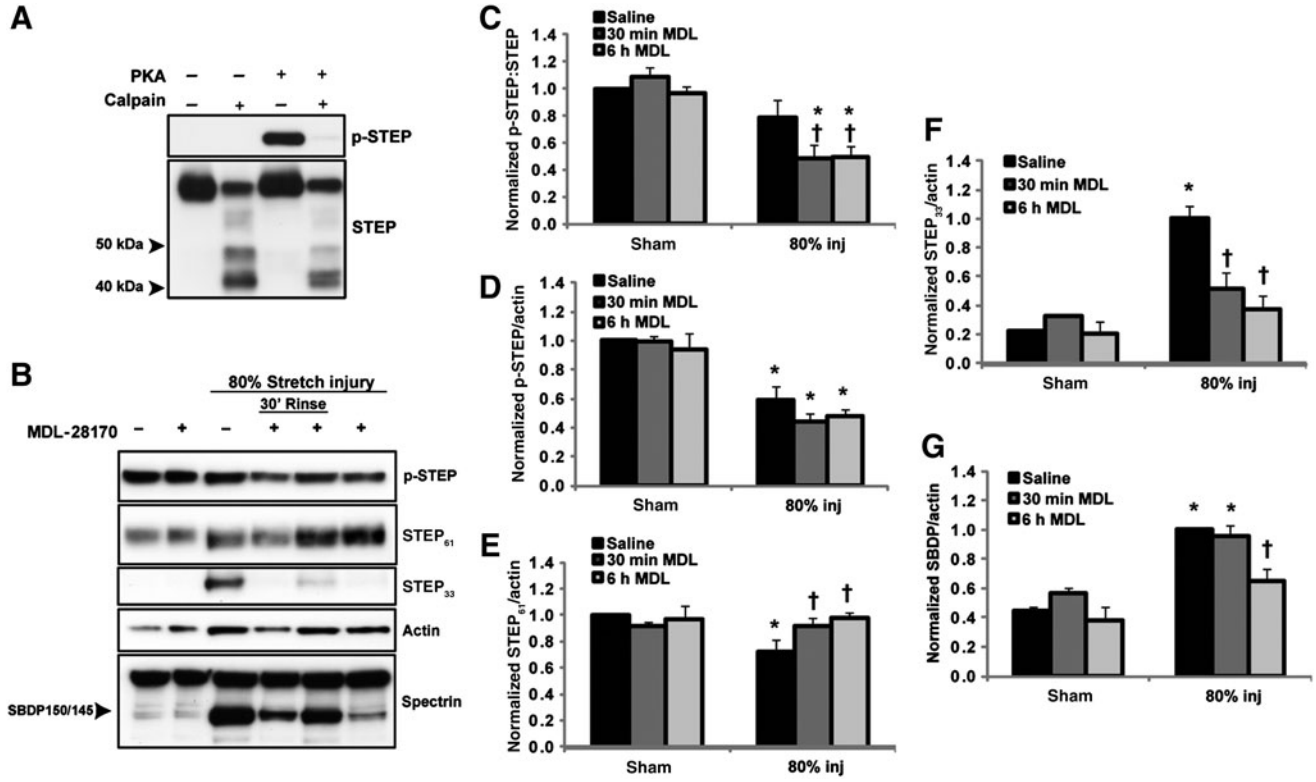

FIG. 3. Phosphorylation does not alter calpain proteolysis of recombinant STEP, while MDL-28170 blocks $STEP_{33}$ formation and increases the relative amount of active STEP after 80% injury in neurons. Recombinant GST-$STEP_{46}$ was phosphorylated by PKA and subsequently cleaved by calpain. (**A**) A representative Western blot shows a similar loss of full-length STEP with calpain inhibition that is independent of its phosphorylation state ($n = 3$). (**B**) A representative Western blot of dissociated cortical lysates injured at 80% peak stretch levels with the calpain inhibitor MDL-28170 (MDL; 5 μM, 15 min), and quantification (**C**–**E**), shows a decrease in phospho-STEP:STEP ratios and blockade of $STEP_{61}$ loss at 6 h after injury. No difference was observed when MDL-28170 was removed 30 min after injury. (**F** and **G**) MDL-28170 blocks $STEP_{33}$ formation, even when removed after 30 min, but only blocks spectrin proteolysis when incubated for 6 h. All band intensities are normalized to time-matched saline uninjured samples, and expressed as the indicated ratios. All values are presented as means ± standard error of the mean (*$p < 0.05$ versus sham; †$p < 0.05$ versus saline; STEP, striatal-enriched tyrosine phosphatase; PKA, protein kinase A; SBDP, breakdown products of spectrin).

To examine the critical window for calpain inhibition of $STEP_{33}$ formation, we injured a separate set of neuronal cultures as described above, but removed MDL-28170 30 min after the injury. Using this shortened (30-min) calpain inhibition protocol, the reduction in $STEP_{33}$ formation at 6 h after injury was comparable to the sustained (6-h) inhibition protocol (Fig. 3B and F). In contrast, spectrin proteolysis was not blocked with the shortened MDL-28170 treatment compared to sustained drug treatment in the same samples (Fig. 3G). Additionally, a decrease in the phospho-STEP:STEP ratio was also observed with the shortened MDL-28170 treatment (Fig. 3C). Together, these data show that calpain activated within the acute time period (< 30 min) underlies $STEP_{33}$ formation at 6 h after stretch injury, while sustained calpain inhibition is necessary for blocking spectrin breakdown.

Synaptic activity is required for STEP phosphorylation after sublethal injury, and potentiates STEP proteolysis after lethal injury

Basal synaptic activity in cultured neurons is critical for the transmission of some phosphorylation-driven signaling pathways, and can even affect the ability of neurons to respond to mechanical injury (Chandler et al., 2001; Geddes-Klein et al., 2006b; Ivanov et al., 2006; Lee et al., 2005). To examine the effect of synaptic activity on STEP phosphorylation and proteolysis after injury, we pretreated cells with tetrodotoxin (TTX; 1 μM, 15 min) and stretch-injured them in the presence of drug for the duration of the experiment to maintain reduced synaptic activity. TTX treatment did not affect injury-induced changes in STEP phosphorylation at the 15-min, 1-h, and 6-h time points (data not shown). However, the presence of TTX reversed the increase in the phospho-STEP:STEP ratio occurring 24 h after 50% stretch injury (Fig. 4A and B). Following 80% stretch injury, TTX treatment did not alter STEP phosphorylation compared to untreated cultures; however, TTX did significantly increase $STEP_{33}$ formation (Fig. 4D). TTX did not alter $STEP_{61}$ expression at either stretch injury level (Fig. 4C). To determine if a similar trend occurred in a phospho-protein known to be sensitive to alterations in synaptic activity (Soriano et al., 2006), we examined changes in cAMP response element-binding protein (CREB) phosphorylation after injury at the 50% and 80% stretch levels. No differences in CREB phosphorylation were observed at 24 h after injury (data not shown), but a similar dependence on synaptic activity for the enhancement of CREB

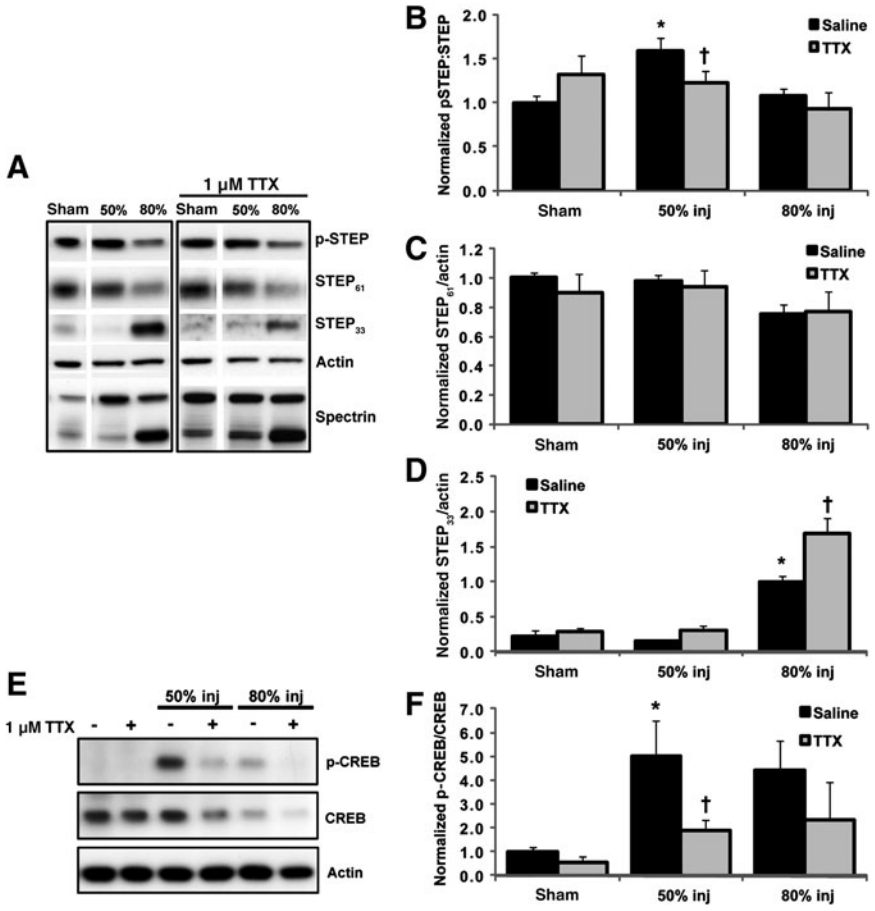

FIG. 4. TTX blocks increased STEP phosphorylation after 50% stretch, and potentiates $STEP_{33}$ formation at 24 h after 80% stretch. Dissociated cortical neurons were pretreated with TTX (1 μM, 15 min), injured at 50% and 80% peak stretch levels, and lysed at 24 h post-injury. (**A**) Representative Western blots, and (**B** and **C**) quantification, show that TTX blocks the increase in phospho-STEP:STEP ratios after 50% stretch injury ($n = 5$–7), with no effect on STEP phosphorylation at 80% stretch levels ($n = 4$–6). (**D**) TTX increases $STEP_{33}$ formation after 80% stretch injury. (**E**) A representative Western blot, and quantification (**F**), show that TTX blocks enhanced CREB phosphorylation (p-CREB) at 6 h after 50% stretch injury ($n = 5$–7), with less robust changes seen after 80% stretch injury ($n = 3$–5). All band intensities are normalized to time-matched, saline or drug-treated, uninjured samples, and expressed as the indicated ratios. All values are presented as means ± standard error of the mean (*$p < 0.05$ versus sham; †$p < 0.05$ versus saline; STEP, striatal-enriched tyrosine phosphatase; TTX, tetrodotoxin; CREB, cAMP response element-binding protein).

phosphorylation was apparent at 6 h after 50% stretch injury (Fig. 4E and F). These data illustrate the importance of synaptic signaling in mediating some, but not all, stretch injury-induced alterations in phosphorylation and proteolysis after sublethal and lethal levels of stretch injury.

Effect of NMDAR or calcineurin on injury-mediated changes is dependent on injury level and duration of drug treatments

STEP phosphorylation and proteolysis changes following *in vitro* chemical stimuli require calcium influx through the NR2B-containing NMDARs, in addition to calcineurin activation (Paul et al., 2003; Poddar et al., 2010; Xu et al., 2009). We evaluated whether inhibition of these pathways with the NMDAR antagonist APV, the NR2B-NMDAR antagonist Ro 25-6981, or the calcineurin inhibitor FK506, could block the short- or long-term stretch-induced changes in STEP. At 15 min after stretch injury, there was no significant effect of any drug on STEP phosphorylation, expression, or proteolysis at the 50% stretch injury level (Fig. 5A and B). After 80% stretch injury, the acute STEP dephosphorylation was blocked with APV (Fig. 5C and D). In comparison, Ro 25-6981 significantly blocked stretch-induced STEP dephosphorylation, but a concurrent increase in $STEP_{61}$ expression resulted in an indistinguishable change in the phospho-STEP:STEP ratio after injury. Surprisingly, FK506 was ineffective at blocking STEP dephosphorylation at this time point. Combined, these data demonstrate that the NMDAR/NR2B-mediated pathway is responsible for the initial STEP dephosphorylation after a mechanical stimulus, similarly to a chemical stimulus (Poddar et al., 2010), yet calcineurin is not involved in STEP dephosphorylation within 15 min of stretch injury.

When considering pathways involved in mediating long-term changes (24 h) after stretch injury, it is important to distinguish between the effect of inhibiting the pathways at the time of injury and the effect of chronic inhibition of those pathways. Since injury-mediated increases in intracellular

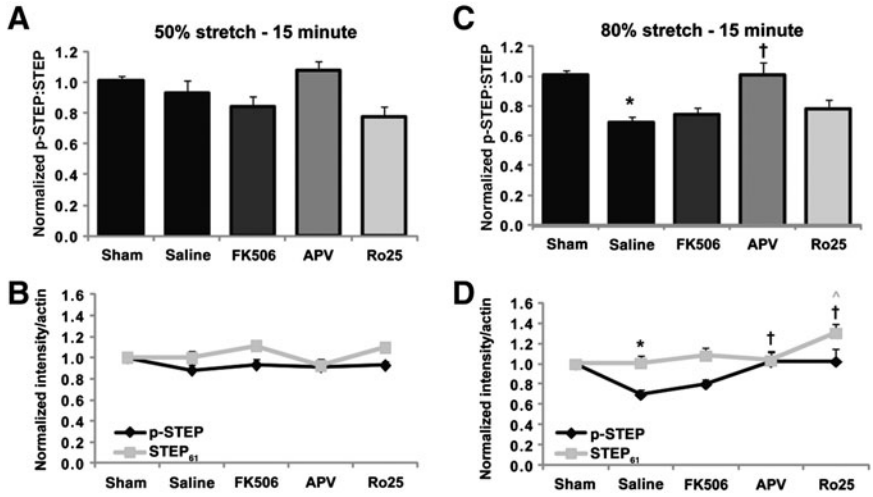

FIG. 5. APV and Ro 25-6981 (Ro25) block acute STEP dephosphorylation at 15 min after 80% stretch. Dissociated cortical neurons were pretreated with 1 μM FK506, 25 μM APV, or 10 μM Ro 25-6981, injured at 50% or 80% peak stretch levels in the presence of drug, and lysed 15 min later ($n = 3$–10/group). Quantified values for (**A** and **C**) phospho-STEP:STEP, and (**B** and **D**) phospho-STEP and $STEP_{61}$, show that APV and Ro 25-6981 block STEP dephosphorylation at the 80% stretch level. FK506 does not have an effect at either stretch level. All band intensities are normalized to time-matched, saline or drug-treated, uninjured samples and expressed as the indicated ratios. All values are presented as means ± standard error of the mean (*$p < 0.05$ versus shams; †$p < 0.05$ versus saline; ^$p < 0.05$ versus saline [$STEP_{61}$]; STEP, striatal-enriched tyrosine phosphatase).

calcium return to baseline levels after 15 min (Spaethling et al., 2008), we compared the effects of blocking NMDAR and calcineurin within the first 30 min after injury, in addition to the 24-h duration of the experiment. At 50% stretch, 30-min incubation with FK506 or APV did not alter phospho-STEP levels or ratios compared to saline-injured samples at 24 h after injury (Fig. 6A and B). Interestingly, Ro 25-6981 treatment for only the first 30 min after injury blocked STEP phosphorylation at this severity at this time point. No $STEP_{33}$ proteolysis occurred at the 50% stretch level in the presence of any of the drugs (Fig. 6C). At 80% stretch injury, FK506, APV, or Ro 25-6981 for the first 30 min post-injury did not produce a change in STEP phosphorylation or $STEP_{61}$ expression (Fig. 6D and E). $STEP_{33}$ formation was slightly reduced with 30-min treatments of FK506 or APV, but was significantly blocked with Ro 25-6981, demonstrating the importance of the immediate (< 30 min) calcium influx through the NR2B-containing NMDA receptors.

Sustained treatment with FK506 and APV after 50% stretch injury reverses the increased phospho-STEP:STEP ratio after injury (Fig. 7A and B). Ro 25-6981 blocked total changes in phospho-STEP, while producing a decrease in $STEP_{61}$ expression that yielded an indistinguishable change in the phospho-STEP:STEP ratio after injury. No $STEP_{33}$ proteolysis occurred at the 50% stretch level in the presence of any of the drugs (Fig. 7C). After 80% stretch injury, sustained inhibition with FK506 and APV further enhanced STEP dephosphorylation compared to saline-injured samples (Fig. 7D and E). Sustained inhibition with Ro 25-6981 did not alter phospho-STEP levels or $STEP_{61}$ expression after injury. Ro 25-6981 completely blocked the robust increase in $STEP_{33}$ formation seen after 80% stretch injury, while APV partially, but significantly, reduced $STEP_{33}$ formation, and FK506 had no effect (Fig. 7F). Taken together, these data demonstrate that the NMDAR and calcineurin mediate long-term changes in STEP phosphorylation and proteolysis after mechanical injury, and are dependent on the timing of pathway inhibition.

Cell death after injury is blocked by NMDAR antagonists and correlates with $STEP_{33}$ formation

Although cell death after 50% and 80% stretch injury in this model has been previously characterized (Geddes-Klein et al., 2006a; Spaethling et al., 2008), the effect of the antagonists used in this study on cell death after *in vitro* stretch injury is unknown. We used a cell death assay with ethidium homodimer and Hoescht to visualize dead and total cell populations, respectively, and quantified the percent of co-labeled (EthHD-positive) cells as a measure of cell death at 24 h after injury. There was no change in neuronal viability at 24 h after 50% stretch injury, regardless of drug treatment (Fig. 8A and B). By comparison, significant increases in cell death were observed 24 h after 80% stretch injury (Fig. 8A and C). FK506 did not block this observed cell death, while APV significantly reduced it compared to saline-injured controls. Ro 25-6981 treatment attenuated cell death to levels similar to APV treatment.

As demonstrated in Figure 7, calpain-mediated $STEP_{33}$ formation after stretch injury only occurs at the higher levels of stretch at which we observed cell death (Fig. 8C). To directly correlate the formation of $STEP_{33}$ with neuronal viability in our cultures, we compared the mean values for $STEP_{33}$ formation with the mean values for cell death at 24 h after stretch injury across all drug treatments in Figures 7 and 8. There was a strong correlation between these measures (Fig. 8D; $R^2 = 0.9275$), even when considering the influence of drug treatments. We did not find any other correlations with the other isoforms of STEP with cell death after injury.

Discussion

The present study is the first examination of STEP phosphorylation or proteolysis changes in cortical neurons after *in vitro* mechanical stretch injury. Patterns of STEP alterations after injury evolve over time, depend on the magnitude of

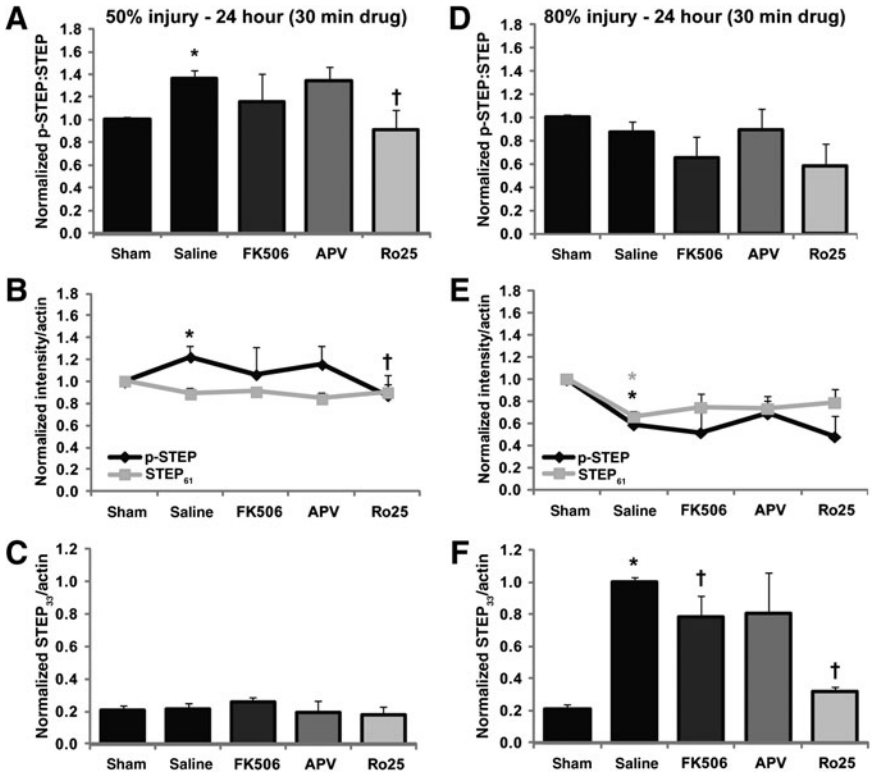

FIG. 6. Shortened Ro 25-6981 treatment reverses STEP phosphorylation and proteolysis at 24 h after injury. Dissociated cortical neurons were pretreated with 1 μM FK506, 25 μM APV, or 10 μM Ro 25-6981 (Ro25), and injured at 50% or 80% peak stretch levels in the presence of drug. The drug was rinsed off 30 min after injury and the cells were lysed 23.5 h later ($n = 3$–6 per group) for Western blot analysis. Quantified band intensities of (**A** and **D**) phospho-STEP:STEP, (**B** and **E**) phospho-STEP, $STEP_{61}$, and (**C** and **F**) $STEP_{33}$, show that 30-min drug treatment was ineffective, except with Ro 25-6981, at blocking the stretch-induced STEP response at both the 50% and 80% levels. All band intensities are normalized to time-matched, saline- or drug-treated, uninjured samples, and expressed as the indicated ratios. All values are presented as means ± standard error of the mean (*$p < 0.05$ versus shams; †$p < 0.05$ versus saline; STEP, striatal-enriched tyrosine phosphatase).

stretch injury, and are influenced by the activity level in cortical neurons. Both the phosphorylation and cleavage of STEP occur via an NMDAR-mediated pathway in stretch injury, in agreement with other models of excitotoxicity (Paul et al., 2003). Collectively, the mechanism and timing of STEP cleavage can be important in determining cell fate after injury, as there is a strong correlation between the extent of cell death and the extent of $STEP_{33}$ formed after injury across all pharmacological treatments used in this study.

Past work demonstrates that STEP expression and activation can be altered by pathophysiological signaling in many models of neuronal dysfunction (Braithwaite et al., 2008; Briggs et al., 2011; Choi et al., 2007; Hicklin et al., 2011; Kurup et al., 2010; Paul and Connor, 2010; Poddar et al., 2010; Saavedra et al., 2011; Xu et al., 2009; Zhang et al., 2010). After injury, we observe a phosphorylation response of STEP that is dependent on injury severity, and a biphasic phosphorylation pattern that is unique to mechanical injury. This biphasic pattern illustrates a potential complexity in decoding the STEP response following injury that is not surprising, since stretch injury mechanisms include immediate changes in the electrophysiological properties of the NMDAR, a slow depolarization persisting for hours, loss of AMPA-receptor desensitization, immediate alterations in network synchrony and activity, and the possible formation of transient pores in the cell membrane (Geddes et al., 2003; Goforth et al., 1999,2011; Singleton and Povlishock, 2004; Spaethling et al., 2008; Tavalin et al., 1995; Zhang et al., 1996).

While there was no evidence of neuronal death at 24 h after stretch injury, we showed that cells experiencing sublethal stretch injury display a progressive increase in $STEP_{61}$ expression and no $STEP_{33}$ formation. Intracellular calcium influx at this injury level occurs primarily through synaptically-localized NMDA receptors (Geddes-Klein et al., 2006b), and is below the calcium load needed for calpain activation. Synaptic activation of glutamate receptors after sublethal injury may mediate the increase of $STEP_{61}$ seen over time, as $STEP_{61}$ expression can be rapidly altered by either translation or dysfunction of the ubiquitin pathway (Paul et al., 2007; Xu et al., 2009; Zhang et al., 2008), and these processes rely on synaptic activity and glutamate receptor activation (Faden et al., 1989; Gong et al., 2006). In addition, mechanical stretch injury can activate mGluR1 and mGluR5 receptors (Faden et al., 2001; Mukhin et al., 1997), which are major contributors to dendritic and synaptic translation pathways, and can mediate STEP translation (Raymond et al., 2000; Zhang et al., 2008). Additionally, the increase in STEP phosphorylation after sublethal stretch injury corresponds with preliminary data showing increased phosphorylation of PKA substrates in the same samples (data not shown), suggesting activation of PKA after sublethal stretch injury. Combined, these data show that sublethal injury to neurons may trigger non-lethal

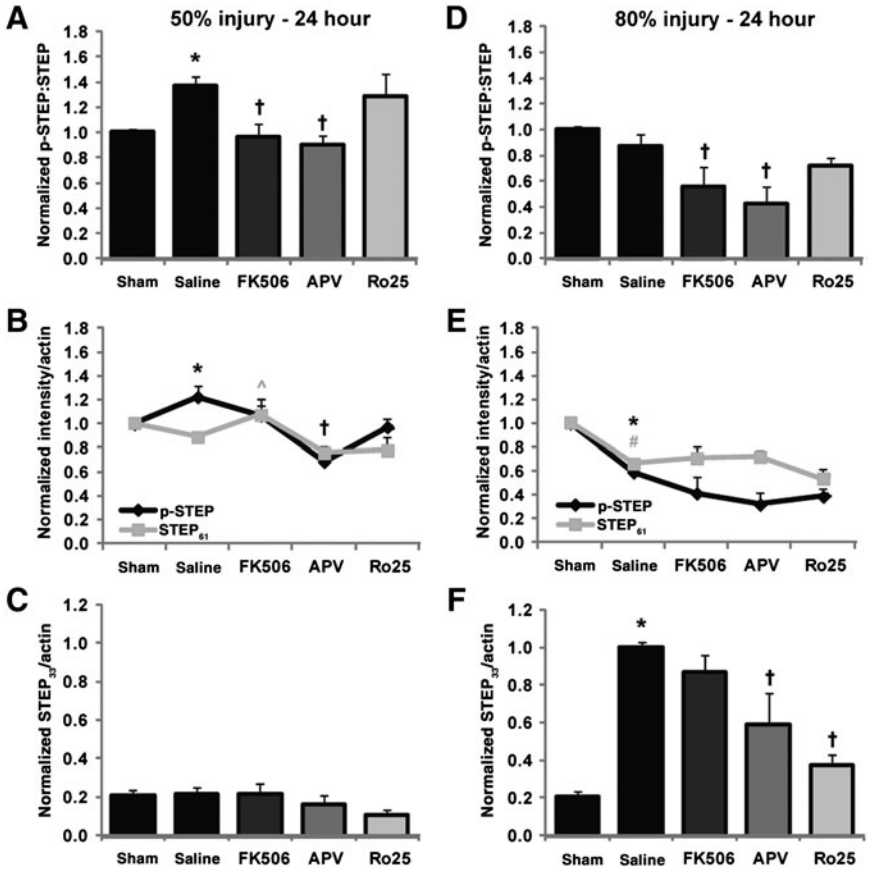

FIG. 7. Sustained APV and FK506 treatment reverses STEP phosphorylation at 24 h after injury. Dissociated cortical neurons were pretreated with 1 μM FK506, 25 μM APV, or 10 μM Ro 25-6981 (Ro25), and stretch-injured at 50% or 80% peak stretch levels in the presence of drug and lysed 24 h later for Western blot analysis ($n = 3$–6 per group). Quantified band intensities for (**A** and **D**) phospho-STEP:STEP, (**B** and **E**) phospho-STEP, $STEP_{61}$, and (**C** and **F**) $STEP_{33}$, show that sustained treatment with APV and FK506 block the stretch response at the 50% and 80% levels. Both NMDA antagonists also significantly blocked $STEP_{33}$ formation after 80% stretch injury. All band intensities were normalized to time-matched, saline- or drug-treated, uninjured samples and expressed as the indicated ratios. All values are presented as means ± standard error of the mean (*$p < 0.05$ versus shams; †$p < 0.05$ versus saline; ^$p < 0.05$ versus saline [$STEP_{61}$]; STEP, striatal-enriched tyrosine phosphatase; NMDA, *N*-methyl-D-aspartate).

downstream pathways that regulate STEP expression and phosphorylation.

The timing and relative balance in STEP phosphorylation shifts when examining stretch injury at levels that produce significant calpain activation and neuronal death. The calpain-mediated $STEP_{33}$ formation observed after lethal stretch injury occurs on the same time scale as its appearance in other excitotoxic insults (Braithwaite et al., 2008; Xu et al., 2009). Our data show that early calpain inhibition leads to sustained protection against $STEP_{33}$ formation at later time points, distinct from the sustained calpain inhibition necessary to block calpain-mediated spectrin breakdown. Spectrin is the most commonly used marker of calpain activation in TBI, yet there is evidence that increased calpain activity can occur in regions that do not exhibit spectrin breakdown (Pike et al., 1998; Saatman et al., 1996). In addition, calpain activation is biphasic and can occur at distinct subcellular locations such as the cell membrane (Buki et al., 1999; Goll et al., 2003; Kilinc et al., 2009; Saatman et al., 2003). Therefore, it is possible that an early wave of calpain activation triggered by *in vitro* stretch injury is initially restricted to a region of the cell where $STEP_{61}$ is anchored (Pelkey et al., 2002). Combined with reports that specific inhibition of $STEP_{33}$ formation protects cells from excitotoxicity (Xu et al., 2009), these data may expose $STEP_{33}$ as a sensitive marker of calpain activation and neuronal viability after injury. Further studies are needed to determine if $STEP_{33}$ formation is critical in the induction of cell death after injury, as our efforts to treat cultures with a calpain inhibitor led to a reduction in $STEP_{33}$ formation, but had variable effects on neuronal viability. We did not observe a correlation between the other isoforms of STEP and viability. Additionally, we show that dephosphorylated STEP is preferentially cleaved by calpain in cultured neurons, but not in *in vitro* studies with recombinant STEP, suggesting that other factors, such as phosphorylation of other residues outside the KIM domain of STEP (Mukherjee et al., 2011), are involved in regulating the ability of calpain to cleave STEP. Therefore, inhibiting STEP proteolysis may create a larger pool of activated STEP, which could be another mechanism of potential neuroprotection of STEP (Choi et al., 2007; Poddar et al., 2010; Saavedra et al., 2011; Xu et al., 2009), and may reveal an interdependence of additional regulatory mechanisms mediating STEP proteolysis.

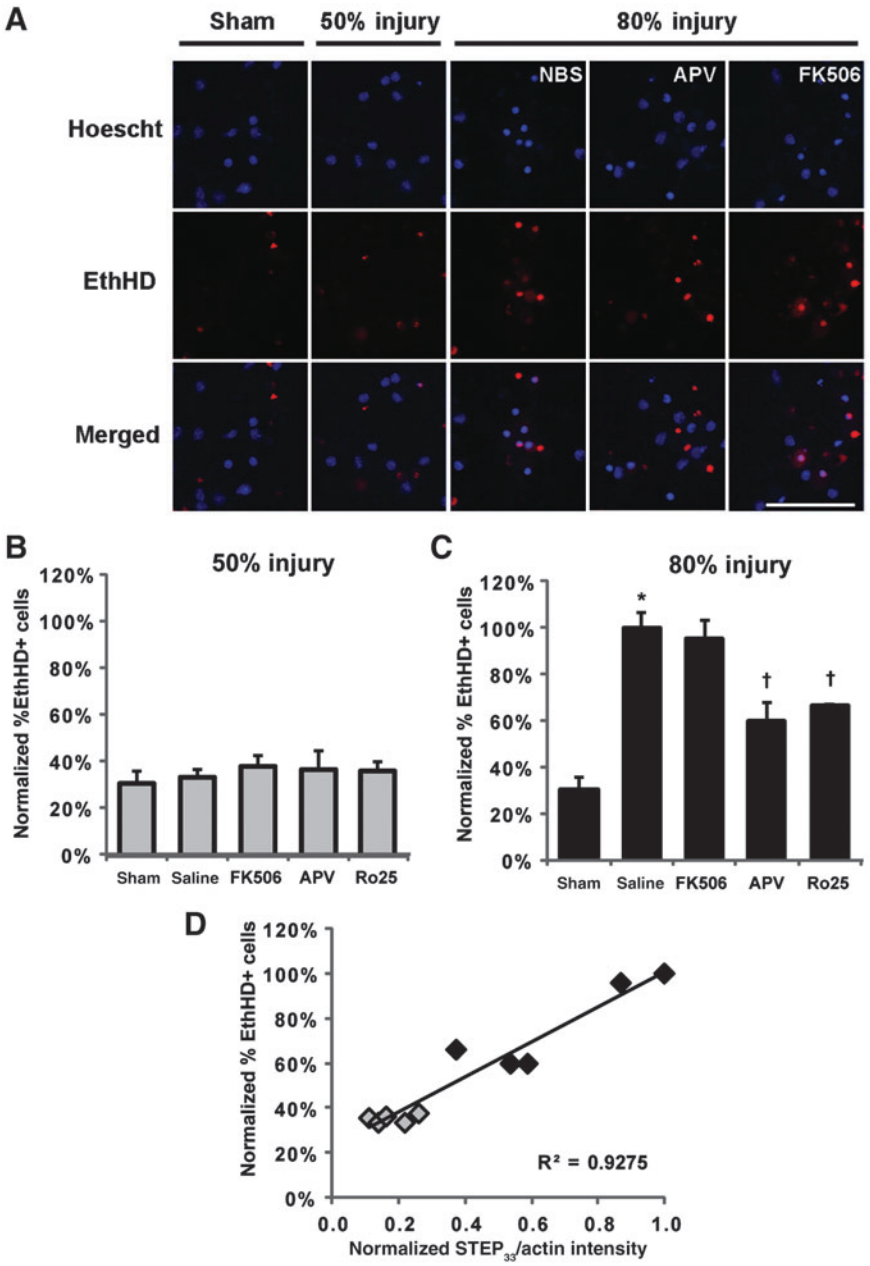

FIG. 8. Cell death at 24 h after 80% stretch via NMDA receptor is strongly correlated with $STEP_{33}$ formation. Dissociated cortical neurons were pretreated with 1 μM FK506, 25 μM APV, or 10 μM Ro 25-6981, injured at 50% or 80% peak stretch levels, and imaged in a Hoescht/ethidium homodimer solution 24 h later. (**A**) Representative photomicrographs show Hoescht, ethidium homodimer (EthHD), and co-labeled cells (Merged) following the indicated stretch level and drug treatment. Quantification of the percent of EthHD-positive cells, normalized to the mean value for cell death in the 80% stretch group from that week of cells, after (**B**) 50% stretch, and (**C**) 80% stretch, shows protection with NMDA antagonists ($n = 3$–14 per treatment group). (**D**) Mean normalized values of cell death as a function of the mean normalized values of $STEP_{33}$ formation after injury shows a positive correlation between $STEP_{33}$ formation and cell death for both 50% stretch-injured (light gray diamonds), and 80% stretch-injured (dark gray diamonds) samples (scale bar = 50 μm). Data are represented as mean ± standard error of the mean (*$p < 0.05$ versus shams; †$p < 0.05$ versus saline; STEP, striatal-enriched tyrosine phosphatase; NMDA, *N*-methyl-D-aspartate; NBS, Neurobasal-based saline solution).

A conserved upstream activation pathway across all stimulation and injury models is NMDAR-mediated STEP dephosphorylation, primarily through the NR2B subunit via a calcineurin/DARPP-32/PP1-mediated pathway (Paul et al., 2003; Poddar et al., 2010; Saavedra et al., 2011; Valjent et al., 2005). Our data show that the NMDAR is also a critical mediator of changes in STEP after mechanical stretch injury, yet suggest that calcineurin does not mediate STEP dephosphorylation within the first 15 min after injury. This non-calcineurin-mediated STEP dephosphorylation may occur through downregulation of PKA, as recently demonstrated in a Huntington's disease model (Saavedra et al., 2011), and

reports show that decreased cAMP levels and PKA activity can occur as early as 15 min after *in vivo* TBI (Atkins et al., 2007; Valjent et al., 2005). Alternatively, STEP may be dephosphorylated by another phosphatase that directly acts on STEP. One serine/threonine phosphatase candidate, PP1, is already implicated in a calcineurin/DARPP-32/PP1-mediated pathway of STEP dephosphorylation (Valjent et al., 2005). Given that PP1 may be activated independently of calcineurin through its interaction with the NMDAR and cytoskeleton (Colbran, 2004; Nishi et al., 2002; Westphal et al., 1999), this phosphatase may be locally activated after stretch injury to subsequently dephosphorylate STEP in the post-acute period. Preliminary data using *in vitro* assays with recombinant STEP and PP1 were inconclusive in confirming a direct action of PP1 on STEP (data not shown), therefore additional studies are needed to identify the specific phosphatase responsible for STEP dephosphorylation immediately following stretch injury.

It is worth noting that our data suggest a potential crosstalk between the long-term pathobiology of axonal damage and synaptic dysregulation through calcineurin. Although we did not observe early calcineurin-mediated changes after mechanical injury, our data showed that calcineurin did contribute to the increase in STEP phosphorylation 24 h after injury. In general, broad changes in calcineurin distribution appear within the traumatically-injured brain (Kurz et al., 2005), with enrichment in the synaptoplasmic compartment over several hours to days after injury. Traumatic axonal injury, the underlying substrate of diffuse axonal injury, is also partly influenced by calcineurin; its inhibition will attenuate the appearance of axonal swelling after TBI (Singleton et al., 2001), and cause an improvement in impaired axonal transport (Marmarou and Povlishock, 2006). Given that axonal damage can occur *in vivo* and not lead to overt neuronal death (Singleton et al., 2002), it would be useful to discern whether moderate, nonlethal injury levels cause axonal swelling and conduction delays within the neural circuits that are influenced by calcineurin activation, given that this activation of calcineurin is important in longer-term changes in STEP phosphorylation. Moreover, it may be valuable to evaluate the coordinated timing of these changes in the axonal and synaptic compartments, to understand if these possible changes evolve in parallel, or if one precedes the other. Discerning if these potential links exist will help determine whether calcineurin represents a broad, common signaling element that influences components of the neural circuitry after injury.

When examining the STEP response at 24 h after stretch injury, we aimed to distinguish between the effects of

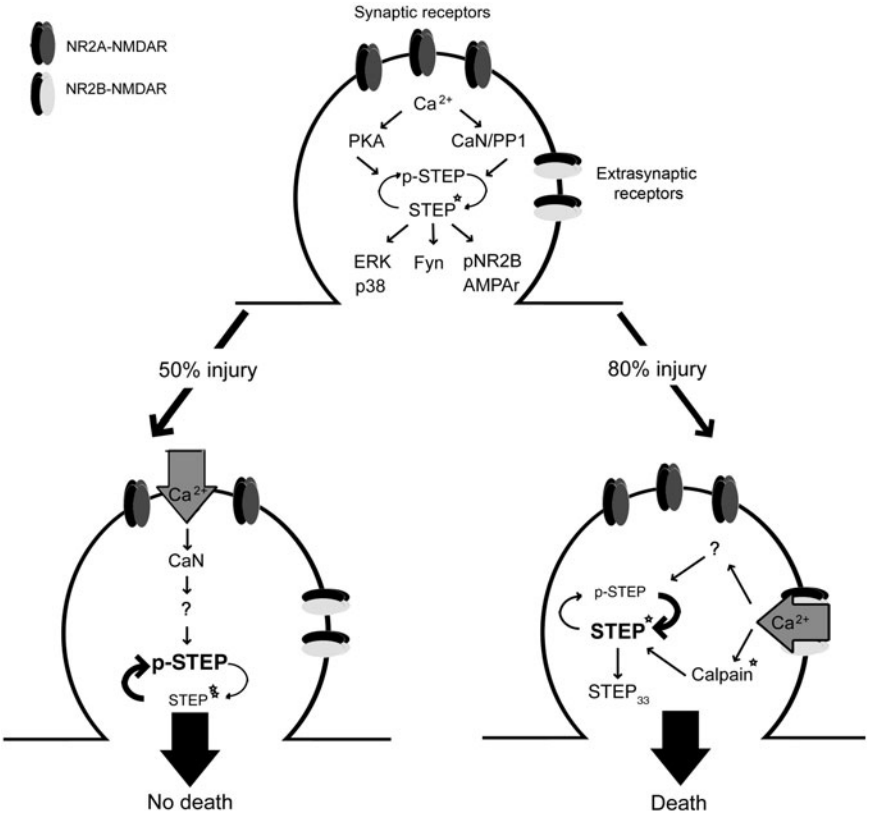

FIG. 9. Illustration of the strain-dependent alterations in STEP phosphorylation and proteolysis following mechanical stretch injury via the NMDAR and calcineurin pathways. Under physiological conditions, the phosphorylation state of STEP is regulated by a balance of PKA and calcineurin (CaN) signaling. Once activated (STEP★), STEP can proceed to affect numerous downstream pathways. After 50% sublethal stretch injury, calcium influx through the synpatic/NR2A-containing NMDARs results in increased STEP phosphorylation that is dependent on calcineurin through an unknown mechanism. After 80% lethal stretch injury, calcium influx through the extrasynaptic/NR2B-containing NMDARs causes STEP dephosphorylation and proteolysis via a non-calcineurin-mediated pathway (STEP, striatal-enriched tyrosine phosphatase; NMDA, *N*-methyl-D-aspartate; PKA, protein kinase A; ERK, extracellular signal-regulated kinases).

blocking the upstream pathways during the post-acute period, and a sustained blockade for the entire post-injury period. We found that activation of the NR2B-containing NMDA receptors within the first 30 min after injury was responsible for the changes in STEP phosphorylation and cleavage observed at 24 h, while blocking all NMDA receptors or calcineurin 30 min after injury had no effect. This finding is consistent with reports that STEP is preferentially localized to the extrasynaptic-containing NMDA receptors (Goebel-Goody et al., 2009), and suggests an importance of STEP anchoring near its site of activation, and a balance between the site of calcium entry and its downstream effects. The aforementioned trend is reversed when drugs remain in the bath solution for the 24-h course of the experiment, as blocking total NMDA receptors or calcineurin, but not NR2B-containing NMDA receptors, eliminated the stretch-induced changes in STEP phosphorylation. Though the mechanism for the observed drug effect at the 50% injury level is unknown, the divergent response in STEP phosphorylation between inhibitors of calcineurin and the NR2B-containing NMDAR shows that calcineurin may not be activated through an NR2B-mediated pathway following stretch injury. This is consistent with our data showing that FK506 failed to block STEP dephosphorylation at 15 min post-injury, and with published reports of an NR2A-NMDAR pathway to calcineurin activation (Izumi et al., 2008). One cofounding variable at the 80% stretch level is the effect of calpain-mediated activation of other downstream substrates of calpain, including calcineurin and the NMDAR. When cleaved by calpain, calcineurin becomes constitutively active, and interactions between the NMDAR and its binding partners can be disrupted, both of which may create unregulated changes in downstream signaling pathways. (Wu et al., 2004,2007; Yuen et al., 2008). This may explain the more complex trends in the data at 24 h after 80% stretch injury. Overall, these data strongly suggest that at least two distinct windows of signaling occur after injury, with an NR2B-NMDAR pathway dominating early, and a total NMDAR/calcineurin pathway playing a role at later time points.

Finally, we show that spontaneous neuronal activity is a critical determinant in the STEP response to 50% stretch injury at 24 h post-injury. TTX inhibits stretch-induced STEP phosphorylation at the sublethal stretch level, similarly to other reports of synaptic activity being necessary to induce phosphorylation-mediated changes after NMDA stimulation (Soriano et al., 2006). Spontaneous neuronal activity tonically activates synaptic NMDA receptors (Hardingham et al., 2002), therefore the ability of TTX to block increases in STEP phosphorylation after sublethal injury builds further evidence that synaptic signaling mediates this change in STEP phosphorylation. The TTX-sensitive increase in CREB phosphorylation after sublethal stretch injury is also consistent with this trend, as CREB is phosphorylated through synaptic NMDAR activation (Hardingham et al., 2002; Papadia et al., 2005). Interestingly, increased CREB phosphorylation via synaptic NMDAR stimulation with bicuculline is linked to a neuroprotective response in cultured neurons (Hardingham et al., 2002), and preliminary data show that bicuculline also induces increased STEP phosphorylation within 15 min of stimulation (data not shown). When combined, these results could suggest that a delayed increase in STEP phosphorylation/inactivation may play a role or be a part of a neuroprotective pathway, as suggested by recent data in a Huntington's disease model (Saavedra et al., 2011).

Our data clearly show that injury severity can serve as a switch for alterations in STEP expression and phosphorylation in cortical neurons after mechanical stretch injury (Fig. 9), and thus a switch in mediating its downstream dephosphorylation of ERK, p38 kinase, and Fyn, in addition to causing internalization of the NMDA and AMPA receptors (Nguyen et al., 2002; Paul et al., 2003; Poddar et al., 2010; Snyder et al., 2005; Zhang et al., 2008). These combined findings may be used to elucidate the direct consequences of STEP activation/inactivation on neuronal fate, and to help develop targeted therapeutic strategies for the detrimental signaling triggered by brain injury. A recent direct link between STEP and the memory deficits that occur in Alzheimer's disease (Zhang et al., 2010) represents an additional potential role of STEP in therapies for TBI, due to the strong similarity in the pathology of these two disorders, and the long-lasting memory deficits afflicting TBI patients (Johnson et al., 2010; Masel and DeWitt, 2010). Combined with the data in this report, further investigation into the role of STEP following *in vivo* TBI may provide critical insight into its regulation of signaling and dysfunction after injury, and may aid in developing STEP-based therapies for excitotoxicity-based disorders.

Acknowledgments

The authors would like to acknowledge Dr. Paul Lombroso (Yale University, New Haven, CT) for the generous donation of the STEP plasmids. Portions of this work were presented at the National Neurotrauma Society and Society for Neuroscience annual meetings. Funds were provided by the National Institutes of Health (grants NS-35712, RO1 HD41699, and P30 HD026979).

Author Disclosure Statement

No competing financial interests exist.

References

Akashi, K., Kakizaki, T., Kamiya, H., Fukaya, M., Yamasaki, M., Abe, M., Natsume, R., Watanabe, M., and Sakimura, K. (2009). NMDA receptor GluN2B (GluR epsilon 2/NR2B) subunit is crucial for channel function, postsynaptic macromolecular organization, and actin cytoskeleton at hippocampal CA3 synapses. J. Neurosci. 29, 10869–10882.

Atkins, C.M., Falo, M.C., Alonso, O.F., Bramlett, H.M., and Dietrich, W.D. (2009). Deficits in ERK and CREB activation in the hippocampus after traumatic brain injury. Neurosci. Lett. 459, 52–56.

Atkins, C.M., Oliva, A.A., Jr., Alonso, O.F., Pearse, D.D., Bramlett, H.M., and Dietrich, W.D. (2007). Modulation of the cAMP signaling pathway after traumatic brain injury. Exp. Neurol. 208, 145–158.

Bell, J.D., Ai, J., Chen, Y., and Baker, A.J. (2007). Mild in vitro trauma induces rapid Glur2 endocytosis, robustly augments calcium permeability and enhances susceptibility to secondary excitotoxic insult in cultured Purkinje cells. Brain 130, 2528–2542.

Bliss, T.V. and Collingridge, G.L. (1993). A synaptic model of memory: long-term potentiation in the hippocampus. Nature 361, 31–39.

Boulanger, L.M., Lombroso, P.J., Raghunathan, A., During, M.J., Wahle, P., and Naegele, J.R. (1995). Cellular and molecular

characterization of a brain-enriched protein tyrosine phosphatase. J. Neurosci. 15, 1532–1544.

Braithwaite, S.P., Adkisson, M., Leung, J., Nava, A., Masterson, B., Urfer, R., Oksenberg, D., and Nikolich, K. (2006). Regulation of NMDA receptor trafficking and function by striatal-enriched tyrosine phosphatase (STEP). Eur. J. Neurosci. 23, 2847–2856.

Braithwaite, S.P., Xu, J., Leung, J., Urfer, R., Nikolich, K., Oksenberg, D., Lombroso, P.J., and Shamloo, M. (2008). Expression and function of striatal enriched protein tyrosine phosphatase is profoundly altered in cerebral ischemia. Eur. J. Neurosci. 27, 2444–2452.

Briggs, S.W., Walker, J., Asik, K., Lombroso, P., Naegele, J., and Aaron, G. (2011). STEP regulation of seizure thresholds in the hippocampus. Epilepsia 52, 497–506.

Buki, A., Okonkwo, D.O., and Povlishock, J.T. (1999). Postinjury cyclosporin A administration limits axonal damage and disconnection in traumatic brain injury. J. Neurotrauma 16, 511–521.

Bult, A., Zhao, F., Dirkx, R., Jr., Raghunathan, A., Solimena, M., and Lombroso, P.J. (1997). STEP: a family of brain-enriched PTPs. Alternative splicing produces transmembrane, cytosolic and truncated isoforms. Eur. J. Cell Biol. 72, 337–344.

Chandler, L.J., Sutton, G., Dorairaj, N.R., and Norwood, D. (2001). N-methyl D-aspartate receptor-mediated bidirectional control of extracellular signal-regulated kinase activity in cortical neuronal cultures. J. Biol. Chem. 276, 2627–2636.

Choi, Y.S., Lin, S.L., Lee, B., Kurup, P., Cho, H.Y., Naegele, J.R., Lombroso, P.J., and Obrietan, K. (2007). Status epilepticus-induced somatostatinergic hilar interneuron degeneration is regulated by striatal enriched protein tyrosine phosphatase. J. Neurosci. 27, 2999–3009.

Colbran, R.J. (2004). Protein phosphatases and calcium/calmodulin-dependent protein kinase II-dependent synaptic plasticity. J. Neurosci. 24, 8404–8409.

Faden, A.I., Demediuk, P., Panter, S.S., and Vink, R. (1989). The role of excitatory amino acids and NMDA receptors in traumatic brain injury. Science 244, 798–800.

Faden, A.I., O'Leary, D.M., Fan, L., Bao, W., Mullins, P.G., and Movsesyan, V.A. (2001). Selective blockade of the mGluR1 receptor reduces traumatic neuronal injury in vitro and improves outcome after brain trauma. Exp. Neurol. 167, 435–444.

Faul, M., Xu, L., and Wald, M. (2010). Traumatic Brain Injury in the United States: Emergency Department Visits, Hospitalizations and Deaths 2002–2006. Atlanta: Centers for Disease Control and Prevention, National Center for Injury Prevention and Control, pps. 1–71.

Fischer, G., Mutel, V., Trube, G., Malherbe, P., Kew, J.N., Mohacsi, E., Heitz, M.P., and Kemp, J.A. (1997). Ro 25-6981, a highly potent and selective blocker of N-methyl-D-aspartate receptors containing the NR2B subunit. Characterization in vitro. J. Pharmacol. Exp. Ther. 283, 1285–1292.

Geddes, D.M., Cargill, R.S., 2nd, and LaPlaca, M.C. (2003). Mechanical stretch to neurons results in a strain rate and magnitude-dependent increase in plasma membrane permeability. J. Neurotrauma 20, 1039–1049.

Geddes-Klein, D.M., Schiffman, K.B., and Meaney, D.F. (2006a). Mechanisms and consequences of neuronal stretch injury in vitro differ with the model of trauma. J. Neurotrauma 23, 193–204.

Geddes-Klein, D.M., Serbest, G., Mesfin, M.N., Cohen, A.S., and Meaney, D.F. (2006b). Pharmacologically induced calcium oscillations protect neurons from increases in cytosolic calcium after trauma. J. Neurochem 97, 462–474.

Goebel-Goody, S.M., Davies, K.D., Alvestad Linger, R.M., Freund, R.K., and Browning, M.D. (2009). Phospho-regulation of synaptic and extrasynaptic N-methyl-d-aspartate receptors in adult hippocampal slices. Neuroscience 158, 1446–1459.

Goforth, P.B., Ellis, E.F., and Satin, L.S. (1999). Enhancement of AMPA-mediated current after traumatic injury in cortical neurons. J. Neurosci. 19, 7367–7374.

Goforth, P.B., Ren, J., Schwartz, B.S., and Satin, L.S. (2011). Excitatory synaptic transmission and network activity are depressed following mechanical injury in cortical neurons. J. Neurophysiol. 105, 2350–2363.

Goll, D.E., Thompson, V.F., Li, H., Wei, W., and Cong, J. (2003). The calpain system. Physiol. Rev. 83, 731–801.

Gong, R., Park, C.S., Abbassi, N.R., and Tang, S.J. (2006). Roles of glutamate receptors and the mammalian target of rapamycin (mTOR) signaling pathway in activity-dependent dendritic protein synthesis in hippocampal neurons. J. Biol. Chem. 281, 18802–18815.

Hardingham, G.E., Fukunaga, Y., and Bading, H. (2002). Extrasynaptic NMDARs oppose synaptic NMDARs by triggering CREB shut-off and cell death pathways. Nat. Neurosci. 5, 405–414.

Hicklin, T.R., Wu, P.H., Radcliffe, R.A., Freund, R.K., Goebel-Goody, S.M., Correa, P.R., Proctor, W.R., Lombroso, P.J., and Browning, M.D. (2011). Alcohol inhibition of the NMDA receptor function, long-term potentiation, and fear learning requires striatal-enriched protein tyrosine phosphatase. Proc. Natl. Acad. Sci. USA 108, 6650–6655.

Hori, N., and Carpenter, D.O. (1994). Transient ischemia causes a reduction of Mg2+ blockade of NMDA receptors. Neurosci. Lett. 173, 75–78.

Hu, Y., Zhang, Y., Venkitaramani, D.V., and Lombroso, P.J. (2007). Translation of striatal-enriched protein tyrosine phosphatase (STEP) after beta1-adrenergic receptor stimulation. J. Neurochem. 103, 531–541.

Ikonomidou, C., and Turski, L. (2002). Why did NMDA receptor antagonists fail clinical trials for stroke and traumatic brain injury? Lancet Neurol. 1, 383–386.

Ivanov, A., Pellegrino, C., Rama, S., Dumalska, I., Salyha, Y., Ben-Ari, Y., and Medina, I. (2006). Opposing role of synaptic and extrasynaptic NMDA receptors in regulation of the extracellular signal-regulated kinases (ERK) activity in cultured rat hippocampal neurons. J. Physiol. 572, 789–798.

Izumi, Y., Tokuda, K., and Zorumski, C.F. (2008). Long-term potentiation inhibition by low-level N-methyl-D-aspartate receptor activation involves calcineurin, nitric oxide, and p38 mitogen-activated protein kinase. Hippocampus 18, 258–265.

Johnson, V.E., Stewart, W., and Smith, D.H. (2010). Traumatic brain injury and amyloid-beta pathology: a link to Alzheimer's disease? Nat. Rev. Neurosci. 11, 361–370.

Kilinc, D., Gallo, G., and Barbee, K.A. (2009). Mechanical membrane injury induces axonal beading through localized activation of calpain. Exp. Neurol. 219, 553–561.

Kumar, A., Zou, L., Yuan, X., Long, Y., and Yang, K. (2002). N-methyl-D-aspartate receptors: transient loss of NR1/NR2A/NR2B subunits after traumatic brain injury in a rodent model. J. Neurosci. Res. 67, 781–786.

Kurup, P., Zhang, Y., Xu, J., Venkitaramani, D.V., Haroutunian, V., Greengard, P., Nairn, A.C., and Lombroso, P.J. (2010). Abeta-mediated NMDA receptor endocytosis in Alzheimer's disease involves ubiquitination of the tyrosine phosphatase STEP61. J. .Neurosci 30, 5948–5957.

Kurz, J.E., Hamm, R.J., Singleton, R.H., Povlishock, J.T., and Churn, S.B. (2005). A persistent change in subcellular

distribution of calcineurin following fluid percussion injury in the rat. Brain Res. 1048, 153–160.

Lee, B., Butcher, G.Q., Hoyt, K.R., Impey, S., and Obrietan, K. (2005). Activity-dependent neuroprotection and cAMP response element-binding protein (CREB): kinase coupling, stimulus intensity, and temporal regulation of CREB phosphorylation at serine 133. J. Neurosci. 25, 1137–1148.

Lin, Y.C., Huang, Z.H., Jan, I.S., Yeh, C.C., Wu, H.J., Chou, Y.C., and Chang, Y.C. (2002). Development of excitatory synapses in cultured neurons dissociated from the cortices of rat embryos and rat pups at birth. J. Neurosci. Res. 67, 484–493.

Liu, Y., Wong, T.P., Aarts, M., Rooyakkers, A., Liu, L., Lai, T.W., Wu, D.C., Lu, J., Tymianski, M., Craig, A.M., and Wang, Y.T. (2007). NMDA receptor subunits have differential roles in mediating excitotoxic neuronal death both in vitro and in vivo. J. Neurosci. 27, 2846–2857.

Loane, D.J., and Faden, A.I. (2010). Neuroprotection for traumatic brain injury: translational challenges and emerging therapeutic strategies. Trends Pharmacol. Sci. 31, 596–604.

Lusardi, T.A., Wolf, J.A., Putt, M.E., Smith, D.H., and Meaney, D.F. (2004). Effect of acute calcium influx after mechanical stretch injury in vitro on the viability of hippocampal neurons. J. Neurotrauma 21, 61–72.

Marmarou, C.R., and Povlishock, J.T. (2006). Administration of the immunophilin ligand FK506 differentially attenuates neurofilament compaction and impaired axonal transport in injured axons following diffuse traumatic brain injury. Exp. Neurol. 197, 353–362.

Masel, B.E., and DeWitt, D.S. (2010). Traumatic brain injury: a disease process, not an event. J. Neurotrauma 27, 1529–1540.

McIntosh, T.K., Vink, R., Soares, H., Hayes, R., and Simon, R. (1990). Effect of noncompetitive blockade of N-methyl-D-aspartate receptors on the neurochemical sequelae of experimental brain injury. J. Neurochem. 55, 1170–1179.

Meaney, D.F., Smith, D.H., Shreiber, D.I., Bain, A.C., Miller, R.T., Ross, D.T., and Gennarelli, T.A. (1995). Biomechanical analysis of experimental diffuse axonal injury. J. Neurotrauma 12, 689–694.

Miller, L.P., Lyeth, B.G., Jenkins, L.W., Oleniak, L., Panchision, D., Hamm, R.J., Phillips, L.L., Dixon, C.E., Clifton, G.L., and Hayes, R.L. (1990). Excitatory amino acid receptor subtype binding following traumatic brain injury. Brain Res. 526, 103–107.

Monyer, H., Burnashev, N., Laurie, D.J., Sakmann, B., and Seeburg, P.H. (1994). Developmental and regional expression in the rat brain and functional properties of four NMDA receptors. Neuron 12, 529–540.

Mukherjee, S., Poddar, R., Deb, I., and Paul, S. (2011). Dephosphorylation of specific sites in the KIS domain leads to ubiquitin-mediated degradation of the tyrosine phosphatase STEP. Biochem. J.

Mukhin, A.G., Ivanova, S.A., and Faden, A.I. (1997). mGluR modulation of post-traumatic neuronal death: role of NMDA receptors. Neuroreport 8, 2561–2566.

Nguyen, T.H., Liu, J., and Lombroso, P.J. (2002). Striatal enriched phosphatase 61 dephosphorylates Fyn at phosphotyrosine 420. J. Biol. Chem. 277, 24274–24279.

Nguyen, T.H., Paul, S., Xu, Y., Gurd, J.W., and Lombroso, P.J. (1999). Calcium-dependent cleavage of striatal enriched tyrosine phosphatase (STEP). J. Neurochem. 73, 1995–2001.

Nishi, A., Bibb, J.A., Matsuyama, S., Hamada, M., Higashi, H., Nairn, A.C., and Greengard, P. (2002). Regulation of DARPP-32 dephosphorylation at PKA- and Cdk5-sites by NMDA and AMPA receptors: distinct roles of calcineurin and protein phosphatase-2A. J. Neurochem. 81, 832–841.

Opitz, T., De Lima, A.D., and Voigt, T. (2002). Spontaneous development of synchronous oscillatory activity during maturation of cortical networks in vitro. J. Neurophysiol. 88, 2196–2206.

Osteen, C.L., Giza, C.C., and Hovda, D.A. (2004). Injury-induced alterations in N-methyl-D-aspartate receptor subunit composition contribute to prolonged 45calcium accumulation following lateral fluid percussion. Neuroscience 128, 305–322.

Palmer, A.M., Marion, D.W., Botscheller, M.L., Swedlow, P.E., Styren, S.D., and DeKosky, S.T. (1993). Traumatic brain injury-induced excitotoxicity assessed in a controlled cortical impact model. J. Neurochem. 61, 2015–2024.

Paoletti, P., and Ascher, P. (1994). Mechanosensitivity of NMDA receptors in cultured mouse central neurons. Neuron 13, 645–655.

Papadia, S., Stevenson, P., Hardingham, N.R., Bading, H., and Hardingham, G.E. (2005). Nuclear Ca2+ and the cAMP response element-binding protein family mediate a late phase of activity-dependent neuroprotection. J. Neurosci. 25, 4279–4287.

Paul, S., and Connor, J.A. (2010). NR2B-NMDA receptor-mediated increases in intracellular Ca2+ concentration regulate the tyrosine phosphatase, STEP, and ERK MAP kinase signaling. J. Neurochem. 114, 1107–1118.

Paul, S., Nairn, A.C., Wang, P., and Lombroso, P.J. (2003). NMDA-mediated activation of the tyrosine phosphatase STEP regulates the duration of ERK signaling. Nat. Neurosci. 6, 34–42.

Paul, S., Olausson, P., Venkitaramani, D.V., Ruchkina, I., Moran, T.D., Tronson, N., Mills, E., Hakim, S., Salter, M.W., Taylor, J.R., and Lombroso, P.J. (2007). The striatal-enriched protein tyrosine phosphatase gates long-term potentiation and fear memory in the lateral amygdala. Biol. Psychiatry 61, 1049–1061.

Paul, S., Snyder, G.L., Yokakura, H., Picciotto, M.R., Nairn, A.C., and Lombroso, P.J. (2000). The Dopamine/D1 receptor mediates the phosphorylation and inactivation of the protein tyrosine phosphatase STEP via a PKA-dependent pathway. J. Neurosci. 20, 5630–5638.

Pelkey, K.A., Askalan, R., Paul, S., Kalia, L.V., Nguyen, T.H., Pitcher, G.M., Salter, M.W., and Lombroso, P.J. (2002). Tyrosine phosphatase STEP is a tonic brake on induction of long-term potentiation. Neuron 34, 127–138.

Pierce, J.E., Smith, D.H., Trojanowski, J.Q., and McIntosh, T.K. (1998). Enduring cognitive, neurobehavioral and histopathological changes persist for up to one year following severe experimental brain injury in rats. Neuroscience 87, 359–369.

Pike, B.R., Zhao, X., Newcomb, J.K., Posmantur, R.M., Wang, K.K., and Hayes, R.L. (1998). Regional calpain and caspase-3 proteolysis of alpha-spectrin after traumatic brain injury. Neuroreport 9, 2437–2442.

Poddar, R., Deb, I., Mukherjee, S., and Paul, S. (2010). NR2B-NMDA receptor mediated modulation of the tyrosine phosphatase STEP regulates glutamate induced neuronal cell death. J. Neurochem. 115, 1350–1362.

Raghupathi, R. (2004). Cell death mechanisms following traumatic brain injury. Brain Pathol. 14, 215–222.

Raghupathi, R., Muir, J.K., Fulp, C.T., Pittman, R.N., and McIntosh, T.K. (2003). Acute activation of mitogen-activated protein kinases following traumatic brain injury in the rat: implications for posttraumatic cell death. Exp. Neurol. 183, 438–448.

Raymond, C.R., Thompson, V.L., Tate, W.P., and Abraham, W.C. (2000) Metabotropic glutamate receptors trigger homo-

synaptic protein synthesis to prolong long-term potentiation. J. Neurosci. 20, 969–976.

Saatman, K.E., Abai, B., Grosvenor, A., Vorwerk, C.K., Smith, D.H., and Meaney, D.F. (2003) Traumatic axonal injury results in biphasic calpain activation and retrograde transport impairment in mice. J. Cereb. Blood Flow Metab. 23, 34–42.

Saatman, K.E., Bozyczko-Coyne, D., Marcy, V., Siman, R., and McIntosh, T.K. (1996). Prolonged calpain-mediated spectrin breakdown occurs regionally following experimental brain injury in the rat. J. Neuropathol. Exp. Neurol. 55, 850–860.

Saavedra, A., Giralt, A., Rue, L., Xifro, X., Xu, J., Ortega, Z., Lucas, J.J., Lombroso, P.J., Alberch, J., and Perez-Navarro, E. (2011). Striatal-enriched protein tyrosine phosphatase expression and activity in Huntington's disease: a STEP in the resistance to excitotoxicity. J. Neurosci. 31, 8150–8162.

Schumann, J., Alexandrovich, G.A., Biegon, A., and Yaka, R. (2008). Inhibition of NR2B phosphorylation restores alterations in NMDA receptor expression and improves functional recovery following traumatic brain injury in mice. J. Neurotrauma 25, 945–957.

Singleton, R.H. and Povlishock, J.T. (2004). Identification and characterization of heterogeneous neuronal injury and death in regions of diffuse brain injury: evidence for multiple independent injury phenotypes. J. Neurosci. 24, 3543–3553.

Singleton, R.H., Stone, J.R., Okonkwo, D.O., Pellicane, A.J., and Povlishock, J.T. (2001). The immunophilin ligand FK506 attenuates axonal injury in an impact-acceleration model of traumatic brain injury. J. Neurotrauma 18, 607–614.

Singleton, R.H., Zhu, J., Stone, J.R., and Povlishock, J.T. (2002). Traumatically induced axotomy adjacent to the soma does not result in acute neuronal death. J. Neurosci. 22, 791–802.

Smith, D.H., Chen, X.H., Pierce, J.E., Wolf, J.A., Trojanowski, J.Q., Graham, D.I., and McIntosh, T.K. (1997). Progressive atrophy and neuron death for one year following brain trauma in the rat. J. Neurotrauma 14, 715–727.

Snyder, E.M., Nong, Y., Almeida, C.G., Paul, S., Moran, T., Choi, E.Y., Nairn, A.C., Salter, M.W., Lombroso, P.J., Gouras, G.K., and Greengard, P. (2005). Regulation of NMDA receptor trafficking by amyloid-beta. Nat. Neurosci. 8, 1051–1058.

Soriano, F.X., Papadia, S., Hofmann, F., Hardingham, N.R., Bading, H., and Hardingham, G.E. (2006). Preconditioning doses of NMDA promote neuroprotection by enhancing neuronal excitability. J. Neurosci. 26, 4509–4518.

Spaethling, J.M., Klein, D.M., Singh, P., and Meaney, D.F. (2008). Calcium-permeable AMPA receptors appear in cortical neurons after traumatic mechanical injury and contribute to neuronal fate. J. Neurotrauma 25, 1207–1216.

Sun, D.A., Deshpande, L.S., Sombati, S., Baranova, A., Wilson, M.S., Hamm, R.J., and DeLorenzo, R.J. (2008). Traumatic brain injury causes a long-lasting calcium (Ca2+)-plateau of elevated intracellular Ca levels and altered Ca2+ homeostatic mechanisms in hippocampal neurons surviving brain injury. Eur. J. Neurosci. 27, 1659–1672.

Tavalin, S.J., Ellis, E.F., and Satin, L.S. (1995). Mechanical perturbation of cultured cortical neurons reveals a stretch-induced delayed depolarization. J. Neurophysiol. 74, 2767–2773.

Valjent, E., Pascoli, V., Svenningsson, P., Paul, S., Enslen, H., Corvol, J.C., Stipanovich, A., Caboche, J., Lombroso, P.J., Nairn, A.C., Greengard, P., Herve, D., and Girault, J.A. (2005). Regulation of a protein phosphatase cascade allows convergent dopamine and glutamate signals to activate ERK in the striatum. Proc. Natl. Acad. Sci. USA 102, 491–496.

von Reyn, C.R., Spaethling, J.M., Mesfin, M.N., Ma, M., Neumar, R.W., Smith, D.H., Siman, R., and Meaney, D.F. (2009). Calpain mediates proteolysis of the voltage-gated sodium channel alpha-subunit. J. Neurosci. 29, 10350–10356.

Westphal, R.S., Tavalin, S.J., Lin, J.W., Alto, N.M., Fraser, I.D., Langeberg, L.K., Sheng, M., and Scott, J.D. (1999). Regulation of NMDA receptors by an associated phosphatase-kinase signaling complex. Science 285, 93–96.

Wu, H.Y., Tomizawa, K., and Matsui, H. (2007). Calpain-calcineurin signaling in the pathogenesis of calcium-dependent disorder. Acta Med. Okayama 61, 123–137.

Wu, H.Y., Tomizawa, K., Oda, Y., Wei, F.Y., Lu, Y.F., Matsushita, M., Li, S.T., Moriwaki, A., and Matsui, H. (2004). Critical role of calpain-mediated cleavage of calcineurin in excitotoxic neurodegeneration. J. Biol. Chem. 279, 4929–4240.

Xu, J., Kurup, P., Zhang, Y., Goebel-Goody, S.M., Wu, P.H., Hawasli, A.H., Baum, M.L., Bibb, J.A., and Lombroso, P.J. (2009). Extrasynaptic NMDA receptors couple preferentially to excitotoxicity via calpain-mediated cleavage of STEP. J. Neurosci. 29, 9330–9343.

Yuen, E.Y., Ren, Y., and Yan, Z. (2008). Postsynaptic density-95 (PSD-95) and calcineurin control the sensitivity of N-methyl-D-aspartate receptors to calpain cleavage in cortical neurons. Mol. Pharmacol. 74, 360–370.

Zhang, L., Rzigalinski, B.A., Ellis, E.F., and Satin, L.S. (1996). Reduction of voltage-dependent Mg2+ blockade of NMDA current in mechanically injured neurons. Science 274, 1921–1923.

Zhang, Y., Kurup, P., Xu, J., Carty, N., Fernandez, S.M., Nygaard, H.B., Pittenger, C., Greengard, P., Strittmatter, S.M., Nairn, A.C., and Lombroso, P.J. (2010). Genetic reduction of striatal-enriched tyrosine phosphatase (STEP) reverses cognitive and cellular deficits in an Alzheimer's disease mouse model. Proc. Natl. Acad. Sci. USA 107, 19014–19019.

Zhang, Y., Venkitaramani, D.V., Gladding, C.M., Zhang, Y., Kurup, P., Molnar, E., Collingridge, G.L., and Lombroso, P.J. (2008). The tyrosine phosphatase STEP mediates AMPA receptor endocytosis after metabotropic glutamate receptor stimulation. J. Neuroscil. 28, 10561–10566.

Address correspondence to:
David F. Meaney, Ph.D.
Department of Bioengineering
University of Pennsylvania
240 Skirkanich Hall
210 South 33rd Street
Philadelphia, PA 19104

E-mail: dmeaney@seas.upenn.edu